ECM1 Attenuates Hepatic Fibrosis by Interfering with Mediators of Latent TGF-β1 Activation

Frederik Link[1], Yujia Li[1], Jieling Zhao[2,3], Stefan Munker[4,5], Weiguo Fan[6], Zeribe C. Nwosu[1,7], Ye Yao[1], Shanshan Wang[8], Chenjun Huang[1,9], Roman Liebe[10], Seddik Hammad[1], Hui Liu[11], Chen Shao[11], Chunfang Gao[9], Bing Sun[12], Natalie J. Török[6], Huiguo Ding[13], Matthias P. A. Ebert[1,14,15], Honglei Weng[1], Peter ten Dijke[16], Dirk Drasdo[2,3], Steven Dooley[1*], Sai Wang[1*]

[1] Department of Medicine II, University Medical Center Mannheim, Medical Faculty Mannheim, Heidelberg University; Mannheim, Germany;

[2] INRIA de Saclay, Palaiseau, France;

[3] IfADo, Dortmund, Germany;

[4] Department of Medicine II, University Hospital, LMU; Munich, Germany;

[5] Liver Center Munich, University Hospital, LMU; Munich, Germany;

[6] Gastroenterology and Hepatology, Stanford University, 300 Pasteur Dr, and VA Palo Alto, CA, USA;

[7] Department of Molecular Biology and Genetics, Cornell University, Ithaca, NY, USA;

[8] Beijing Institute of Hepatology, Beijing You'an Hospital, Capital Medical University, Beijing, China.

[9] Department of Clinical Laboratory Medicine Center, Yueyang Hospital of Integrated Traditional Chinese ans Western Medicine, Shanghai University of Traditional Chinese Medicine, Shaihai, China.

[10] Clinic of Gastroenterology, Hepatology and Infectious Diseases, Otto-von-Guericke-University, Magdeburg, Germany;

[11] Department of Pathology, Beijing You'an Hospital, Affiliated with Capital Medical University, Beijing, China;

[12] State Key Laboratory of Cell Biology, Shanghai Institute of Biochemistry and Cell Biology, Center for Excellence in Molecular Cell Science, Chinese Academy of Sciences, Shanghai, China;

[13] Department of Gastroenterology and Hepatology, Beijing You'an Hospital, Affiliated with Capital Medical University, Beijing, China;

[14] Molecular Medicine Partnership Unit, European Molecular Biology Laboratory, Heidelberg, Germany;

[15] DKFZ-Hector Cancer Institute at the University Medical Center, Mannheim, Germany;

[16] Oncode Institute and Department of Cell and Chemical Biology, Leiden University Medical Center; Leiden, Netherlands;

Corresponding authors

Prof. Dr. rer. nat. Steven Dooley

Department of Medicine II, Section Molecular Hepatology, University Medical Center Mannheim, Medical Faculty Mannheim, Heidelberg University, Germany

Theodor-Kutzer-Ufer 1-3

68167 Mannheim
E-mail: steven.dooley@medma.uni-heidelberg.de
Tel: +49 621-383-3768
Dr. sc. hum. Sai Wang
Department of Medicine II, Section Molecular Hepatology, University Medical Center Mannheim, Medical Faculty Mannheim, Heidelberg University, Germany
Theodor-Kutzer-Ufer 1-3
68167 Mannheim
E-mail: sai.wang@medma.uni-heidelberg.de
Tel: +49-621-383-5595

Key word: ECM1, LTGF-β activation, TSP, ADAMTS, MMP, liver fibrosis
Number of figures and tables: 8 figures
Competing interests: The authors have declared that no competing financial interests exists.
Financial support
This work was supported by the Deutsche Forschungsgemeinschaft (DFG) [grant number DO 373/20-1 to SD], Federal Ministry of Education and Research (BMBF) Program LiSyM-HCC, [grant number PTJ-031L0257A to SD], the Stiftung Biomedizinische Alkohol-Forschung, [grant number 73000350], and HiChol [01GM1904A to RL].

Author contributions
Conceptualization: SD, SW
Methodology: FL, SW, YL, JZ, DD, SM, WF, ZCN, YY, CH, SH
Investigation: FL, SW, YL, JZ, SM, ZCN, WF, SW, YY, HL, CS, DD
Visualization: FL, SW, JZ, DD, YY, CH
Funding acquisition: SD
Project administration: SD, SW, FL
Supervision: SW, SD
Writing - Original: FL, SW, SD
Writing - review: FL, SW, SD, JZ, DD, PTD, ZCN, RL, HW, ME, NJT, BS, HD, CG
SW and SD acted as guarantors.

Acknowledgments
We acknowledge the support of the LIMa Live Cell Imaging at Microscopy Core Facility Platform Mannheim (CFPM).

Abbreviations

aHSC: activated HSCs

aMph: Ly6C+ and Ly6C- macrophages

aTGF-β: active TGF-β

AAV: adeno associated virus

ADAMTS1: A disintegrin and metalloproteinase with thrombospondin motifs 1

ASH: Alcoholic steatohepatitis

CCl_4: carbon tetrachloride

CLD: Chronic liver disease

ECM1: Extracellular matrix protein 1

FXR: Farnesoid X recptor

HCC: Hepatocellular carcinoma

HSC: Hepatic stellate cell

IF: Immunofluorescence staining

IHC: Immunohistochemistry staining

i.v.: intravenous

i.p.: intraperitoneal

KO: knockout

KQFK: Lysine-Glutamine-Phenylalanine-Lysine

KRFK: Lysine-Arginine-Phenylalanine-Lysine

KTFR: Lysine-Threonine-Phenylalanine-Arginine

LAP: Latency associated peptide

LTGF-β (1): Latent transforming growth factor-β (1)

MMP-2: matrix metalloproteinase-2

MMP-9: matrix metalloproteinase-9

NAFLD: Non-alcoholic fatty liver disease

NASH: Non-alcoholic steatohepatitis

PPIA: peptidylprolyl Isomerase A

PSR: picrosirius red

ROS: reactive oxygen species

SEAP: secreted alkaline phosphatase

TGF-β1: Transforming growth factor-β 1

TSP-1: Thrombospondin 1

RT-qPCR: real-time quantitative polymerase chain reaction

WT: wild type

Abstract

Objective:

Extracellular Matrix Protein 1 (ECM1) serves as a gatekeeper of hepatic fibrosis by maintaining transforming growth factor-β1 (TGF-β1) in its latent form. ECM1 knockout (KO) causes latent (L) TGF-β1 activation, resulting in hepatic fibrosis with rapid mortality. In chronic liver disease (CLD), ECM1 decreases with increasing CLD severity. We investigate the regulatory role of ECM1 in TGF-β1 bioavailability and its impact on CLD progression.

Design:

RNAseq was performed to analyze hepatic gene expression. Functional assays were performed using hepatic stellate cells (HSCs), *Ecm1*-KO and *Fxr*-KO mice, patient liver tissue, and computer simulations.

Results:

Expression of LTGF-β1 activators, including thrombospondins (TSPs), ADAMTS proteases, and matrix metalloproteinases (MMPs) increased along with pro-fibrotic gene expression in liver tissue of *Ecm1*-KO mice. In HSCs, overexpression of ECM1 prevented TSP-1-, ADAMTS1-, and MMP-2/9-mediated LTGF-β1 activation. *In vitro* interaction assays demonstrated that ECM1 inhibited LTGF-β1 activation by interacting with TSP-1 and ADAMTS1 via their respective, intrinsic KRFK or KTFR amino acid sequences, and by suppressing MMP-2/9 proteolytic activity. In mice, ECM1 overexpression attenuated KRFK-induced LTGF-β1 activation, while KTFR treatment reversed *Ecm1*-KO- and *Fxr*-KO-mediated liver injury. In patients with CLD, ECM1 expression was inversely correlated with TSP-1, ADAMTS1, MMP-2/9 expression and LTGF-β1 activation. And these results were complemented by a computational compartment model representing the key network of cellular phenotypes and predicted interactions in liver fibrogenesis.

Conclusion:

Our findings underscore the hepatoprotective effect of ECM1, which interferes with mediators of LTGF-β1 activation, suggesting ECM1 or its representative peptide as potential anti-fibrotic therapies in CLD.

248 words

132 **What is already known on this topic?**

133 ➢ ECM1 expression is negatively correlated with CLD progression.

134 ➢ ECM1 maintains liver homeostasis by keeping TGF-β1 latency.

135 **What this study adds?**

136 ➢ ECM1 inhibits LTGF-β1 activation through interfering with key activators, including
137 TSP-1, ADAMTS1, MMP-2, and MMP-9.

138 ➢ ECM1 interacts with TSP-1 and ADAMTS1 via their respective, intrinsic KRFK or
139 KTFR amino acid motifs, and suppresses MMP-2/9 proteolytic activity.

140 ➢ *In vivo*, ECM1 overexpression mitigates KRFK peptide-induced LTGF-β1 activation,
141 while KTFR peptide rescues *Ecm1*-KO- and *Fxr*-KO-induced liver injury.

142 ➢ ECM1 expression inversely correlates with TSP-1, ADAMTS1, MMP-2/9 expression and
143 LTGF-β1 activation in CLD patients.

144 **How might this study affect research, practice or policy?**

145 ➢ Considering severe adverse effects associated with anti-fibrotic treatments utilizing TGF-
146 β1 receptor inhibitors, our findings indicate that restoration of ECM1 expression or
147 phenocopying peptides might represent a novel and safe route to urgently needed anti-
148 fibrotic therapies in CLD.

Introduction

Hepatic fibrosis is the main clinical outcome of CLD, paving the ground for the development of liver cirrhosis and hepatocellular carcinoma (HCC) [1]. Fibrotic diseases constitute an increasing global health burden, with no specific treatments available [2]. Extracellular matrix protein 1 (ECM1), a secreted glycoprotein [3], is essential for the maintenance of tissue homeostasis [4, 5]. In the liver, a gradual decrease of ECM1 expression has been associated with progressive hepatic fibrosis [6]. Complete depletion of ECM1 in mice results in severe and lethal liver fibrosis accompanied by drastically upregulated transforming growth factor-β (TGF-β)1 signaling [6]. ECM1 was also discovered to be the third most abundant gene encoding a secreted protein in quiescent hepatic stellate cells (HSC) and shown to be downregulated during their transdifferentiation to fibrogenic myofibroblasts [7], suggesting that quiescent HSCs are important providers of ECM1 to maintain hepatic homeostasis.

Targeting TGF-β1 signaling is considered a risky therapeutic strategy in many organs due to its heterogenous and contextual cellular functions [8, 9]. This includes the liver, where loss or complete inhibition of TGF-β1 results in developmental disorders, deleterious multi-organ inflammation, and early postnatal death [10], while excessive TGF-β1 signaling in CLD causes fibrosis progression and tumor metastasis [11, 12, 13]. Due to its broad range of functions and effects, the bioavailability of TGF-β1 is tightly controlled [14]. Upon intracellular synthesis, TGF-β1 is secreted and stored covalently attached to ECM molecules as an inactive protein complex termed latent TGF-β1 (LTGF-β1) [15]. Activation of LTGF-β1 involves a range of mechanisms [14], including integrins [16, 17], proteases [18], reactive oxygen species (ROS) [19], mechanical force [16, 20], and various other physical and chemical cues [21, 22]. Progressive hepatic fibrosis is driven by increasing levels of active TGF-β1 [23, 24]. Targeting the active TGF-β1 molecule through direct inhibition has not proven feasible due to severe adverse effects. Therefore, our current research aimed at uncovering the regulatory mechanisms behind the bioavailability of TGF-β1 to develop safer anti-fibrotic strategies [14]. Specifically, we examined whether and how ECM1 prevents LTGF-β1 activation *in vitro* and *in vivo*. Moreover, we complemented our analysis by a computational model that implements major cell types and inter-/intracellular communications that may be affected by changes in the concentration of ECM1.

Results

Ecm1 depletion induces mediators able to activate LTGF-β1 and hepatic fibrogenesis.

181 *Ecm1* depletion (*Ecm1*-KO) in mice leads to hepatic fibrosis and rapid mortality at the age of
182 8-12 weeks [6]. To investigate mechanisms involved in *Ecm1*-KO-induced liver injuries, liver
183 tissue from WT and *Ecm1*-KO mice at 2, 5, and 8 weeks of age (n = 3) was collected for
184 RNAseq analyses. As TGF-β1 is already known to be the central mediator of liver injury in
185 *Ecm1*-KO mice [6], we analyzed changes in gene transcription specifically in the context of
186 this cytokine. Consequently, we sought for the expression of candidate factors that are
187 capable of LTGF-β1 activation in young (2-weeks-old) *Ecm1*-KO mice. We discovered that
188 *Ecm1*-KO mice expressed considerably higher levels of thrombospondins (*Tsps*) and several
189 *Adamts* proteases, including *Adamts4*, *Adamtsl2*, *Thbs1* (*Tsp1*), *Adamts9*, *Thbs2* (*Tsp2*),
190 *Adamts2*, *Adamts1* **(Figure 1A)**, some of which are known to activate LTGF-β1 or interact
191 with the latency associated peptide (LAP) of LTGF-β1 [25, 26]. Additionally, numerous
192 matrix metalloproteases (*Mmps)* known to activate LTGF-β1 *in vitro* [27] including *Mmp-2*,
193 *Mmp-8*, *Mmp-13*, *Mmp-9* were upregulated in *Ecm1*-KO mice **(Figure 1A)**. The chord
194 diagram demonstrated that these elevated molecues are components of the extracellular
195 matrix (ECM) and implicated in ECM (re-)organization due to their peptidase or proteolytic
196 activity **(Figure 1B)**, hence supporting their critical role in tissue remodeling during fibrosis.
197 Furthermore, networking analyses showed that the majority of these Tsps, Adamts proteases,
198 and Mmps share protein domains, while some of them also show co-localization, physical
199 interaction, co-regulated pathways, and genetic interactions **(Figure 1C)**. Knowing its direct
200 effect on integrin activity, we hypothesized that ECM1 may be a modulator of these LTGF-β1
201 activators, eventually possibly, through binding to shared protein domains. To further
202 investigate the correlation of these factors with LTGF-β1 activation in the setting of *Ecm1*
203 depletion, we analyzed their participation in functional pathways and found notable
204 upregulation in endodermal cell differentiation, cell migration, and vascular smooth muscle
205 cell proliferation in *Ecm1*-KO mice, all well-known as regulated by means of TGF-β
206 signaling **(Figure 1D, E)**, suggesting that all upregulated factors are substantially involved in
207 LTGF-β1 activation when ECM1 is depleted. Indeed, when *Ecm1* was knocked out,
208 expression of Tsp-1, Adamts1, Mmp-2 and -9 were all increased on mRNA and protein level
209 **(Figure 1F, G)**.
210 Next, we employed an antibody that selectively recognizes the TGF-β1 latency associated
211 peptide (LAP) breakdown product (LAP-D R58), which is retained in the ECM following
212 LTGF-β1 activation. Immunohistochemistry (IHC) staining showed that, compared to WT
213 mice, there was enhanced LTGF-β1 activation in the liver tissue of *Ecm1*-KO mice, with
214 LAP-D R58 expression detected in the (peri-)sinusoidal area **(Figure 1H)**. Consistent with the

215 profibrogenic effects of TGF-β1, many genes encoding for prominent matrisomal proteins,
216 such as collagen type 1 (*Col1α1*, *Col1α2*), collagen type 3 (*Col3α1*), collagen type 5 (*Col5α1*,
217 *Col5α2*, *Col5α3*), collagen type 6 (*Col6α1*, *Col6α2*, *Col6α3*), and the HSC activation marker
218 *Acta2* were significantly upregulated in *Ecm1*-KO mice, and remained elevated over the
219 investigated time course **(Figure 1I)**. Intriguingly, *Col27a1*, *Col4a3*, and *Col15a* distinguish
220 themselves from the aforementioned fibrillous collagens, as they are important structural
221 components of the ECM in healthy livers and were decreased in *Ecm1*-KO mice at 5 or 8
222 weeks, further indicating ECM1's substantial role in liver tissue homeostasis **(Figure 1I,**
223 **bottom left, 2 panels)**. Given that HSCs were identified as the primary producers of TGF-β1
224 and its activators, we analyzed mRNA expression for our target genes in primary quiescent
225 and activated HSCs isolated from control and CCl_4-treated mice (n=3) from the Gene
226 Expression Omnibus (GEO) DataSets GSE149508 [28]. Specifically, compared to quiescent
227 HSCs, *Ecm1* exhibited a noteworthy downregulation, whereas *Tsps*, *Adamts proteases*, *Mmps*,
228 and fibrotic *collagens* demonstrated substantial upregulation in activated HSCs **(Figure 1J)**,
229 in line with the results in *Ecm1*-KO mice.
230 To summarise, ECM1 depletion causes notable upregulation of known activators of LTGF-β1,
231 including TSPs, ADAMTS proteases, and MMPs, which may subsequently mediate activation
232 of large amounts of LTGF-β1 deposited in the ECM, causing the lethal hepatic fibrosis seen
233 in *Ecm1*-KO mice.

234 **ECM1 inhibits αvβ6 integrin-mediated LTGF-β1 activation**

235 Our previous study showed that ECM1 inhibits αvβ6 integrin-mediated LTGF-β1 activation
236 by interference with its binding to LTGF-β1's RGD motif [6]. To mechanistically study the
237 inhibitory effect of ECM1 on LTGF-β1 activation in further detail, we set up an *in vitro*
238 system comprising HSCs and the TGF-β/SMAD signaling reporter cell line MFB-F11, in
239 which the active TGF-β in the supernatant of HSCs can be measured by incubating the
240 conditioned media with MFB-F11 cells and performing a SEAP (secreted alcaline
241 phosphatase) activity assay **(Figure 2A)**, which is more sensitive than a TGF-β1 ELISA
242 (**Figure S1A, B**). For functional proof of the assay, we tested the cells with αvβ6 integrin as a
243 positive control for LTGF-β1 activation. As anticipated, pre-treatment of LX-2 HSCs and
244 primary human (ph) HSCs that predominantly produce TGF-β1 [29, 30] with 100ng/ml
245 recombinant ECM1 (rECM1) or transfection with an ECM1 plasmid (V-ECM1; LX-2 HSCs)
246 (pcDNA3.1 was transfected as a control plasmid), before adding αvβ6 integrin, both
247 significantly reduced TGF-β signaling reporter activation in MFB-F11 cells, as compared to

248 controls **(Figure 2B)**. 100 ng/ml rECM1 was selected from an experiment using different
249 concentrations of rECM1 and LTGF-β1 activation by SEAP assay (**Figure S1C**). ECM1's
250 successful overexpression was checked by RT-qPCR, immunoblotting, and IF staining
251 (**Figure S2**). Our data suggested that ectopic, ECM1-dependent inhibition of αvβ6 integrin-
252 mediated LTGF-β1 activation can be robustly documented with the SEAP assay. In line,
253 mRNA and protein expression of hepatic fibrosis markers *ACTA2*/α-SMA, COL1A1,
254 COL3A1, and TIMP1 were decreased ECM1-dependently **(Figure 2C, D)**. Lastly, the
255 inhibitory effect of ECM1 on αvβ6 integrin-mediated LTGF-β1 activation was detected by
256 measuring the TGF-β1 LAP-D (R58) fragment using IF staining and quantitative image
257 analysis **(Figure 2E)**.

258 **ECM1 inhibits TSP-1/ADAMTS1/MMP-2/MMP-9-mediated LTGF-β1 activation**

259 Directed by our gene expression data **(Figure 1A, F, G)** and previous literature, we selected
260 four activating mediators (namely, TSP-1, ADAMTS1, MMP-2, and MMP-9) to further study
261 whether ECM1 can prevent LTGF-β1 activation in such a broad and overarching manner. LX-
262 2 HSCs and phHSCs were incubated with rECM1 or transfected with V-ECM1 (LX-2 HSCs)
263 followed by treatment with/without TSP-1, ADAMTS1, MMP-2, or MMP-9 (pcDNA3.1 was
264 used as a control). SEAP activity assay results exemplified that incubation with the activators
265 increased the concentration of active TGF-β1 in conditioned supernatants of LX-2 HSCs as
266 well as phHSCs. LTGF-β1 activation was completely abrogated by prior treatment with
267 rECM1 or upon ECM1 overexpression, assessed for active TGF-β in the supernatant by
268 SEAP assays **(Figure 3A)**. In line with these findings, the expression of fibrosis markers on
269 mRNA level induced by TSP1, ADAMTS1, MMP-2, or MMP-9, including *ACTA2*, *COL1A1*,
270 *COL3A1*, or *TIMP1*, were blunted when rECM1 or V-ECM1 were administered in advance to
271 phHSCs or LX-2 HSCs **(Figure 3B-D)**. We also confirmed ECM1's inhibitory effect by
272 showing that it reduced expression of fibrosis markers on protein level, compared to the
273 groups treated with one of the four activators, as tested by immunoblotting **(Figure 3E)**. The
274 findings were further underscored by the observed loss of TGF-β1 LAP-D (R58)
275 immunofluorescence, when ECM1 was overexpressed in presence of TSP-1, ADAMTS1,
276 MMP-2, or MMP-9 in LX-2 HSCs **(Figure 3F)**.

277 **ECM1 inhibits LTGF-β1 activation via interaction with TSP-1/ADAMTS1's motifs**
278 **KRFK/KTFR and modulation of MMP-2/9`s proteolytic activity**

279 To confirm the role of ECM1 as a direct and broad inhibitor of multiple LTGF-β1 activators
280 and to exclude the presence of confounding effects from other TGF-β isoforms or other
281 relevant signals in HSCs, we incubated MFB-F11 cells with 4ng/ml recombinant (r)LTGF-β1,
282 followed by treatment with each of the four LTGF-β1 activating mediator, alone or together
283 with rECM1. Again, the presence of rECM1 prevented rLTGF-β1 activation by TSP-1-,
284 ADAMTS1-, MMP-2 and MMP-9, as indicated by the *in vitro* SEAP assay results **(Figure**
285 **4A)**. To delve further into how ECM1 inhibits LTGF-β1 activation induced by the above
286 mediators, we performed protein-protein and protein-peptide interaction studies.
287 Immunoprecipitation (IP) analyses illustrated that ECM1 interacted with TSP-1, ADAMTS1,
288 and mature forms of MMP-2 and MMP-9 in LX-2 HSCs that were cultured for 72h **(Figure**
289 **4B)**. *In vitro* pull-down assays using purified recombinant proteins confirmed that ECM1
290 directly bound to TSP-1 (**Figure 4C**), ADAMTS1 (**Figure 4D**), MMP-2 (**Figure 4E**), and
291 MMP-9 (**Figure 4F**). The respective whole immunoblotting membranes can be found in
292 **Figures S3A-D**. **Figure S3E** demonstrated that ECM1 directly interacted with rLTGF-β1 in
293 the *in vitro* pull-down assay. However, it did not affect rLTGF-β1 activation (**Figure 4A, G**,
294 the first and third column in each histogram) thus, ruling out any direct inhibitory effect of
295 ECM1 on LTGF-β1 activation. Incubation of MFB-F11 cells with rECM1 and active TGF-β1
296 did not affect TGF-β1-induced SEAP signal, which suggests that ECM1 does not directly
297 antagonize active TGF-β1 (**Figure S3F**). Additionally, the Alphafold3 system [31] provided
298 structure predictions on the potential localization of interactions between ECM1 and TSP-1,
299 ADAMTS1, MMP-2, MMP-9, or LTGF-β1 (**Figure S4A-E**), using their full-length target
300 proteins as input sequences.
301 It is known that TSP-1 and ADAMTS1 activate LTGF-β1 through an interaction of their
302 respective KRFK [32] or KTFR [33] amino acid motifs. Both motifs are said to induce a
303 conformational change in the LTGF-β1 molecule to release the active TGF-β1 ligand from its
304 complex without the need for additional proteolysis. Further, there is data indicating TSP1`s
305 KRFK peptide in being sufficient to activate LTGF-β1, while the KTFR peptide within the
306 full ADAMTS1 protein is necessary, but by itself not sufficient for LTGF-β1 activation. In
307 fact, the KTFR peptide displays a competitive inhibition of ADAMTS1-mediated LTGF-β1
308 activation when used in a recombinant form [26, 33]. To identify how ECM1 functionally
309 integrates into these seemingly opposing effects of the KRFK and KTFR peptides on LTGF-
310 β1 activation, we tested chemically synthesized KRFK and KTFR peptides in two distinct
311 contexts. An inert KQFK peptide was used as a negative control. MFB-F11 cells were
312 incubated with rLTGF-β1 followed by treatment of rECM1 and/or KRFK peptide to

313 demonstrate that rECM1 caused marked inhibition of KRFK peptide-induced effects on the
314 TGF-β reporter assay activity **(Figure 4G)**. Due to different properties of the ADAMTS1-
315 KTFR motif, MFB-F11 cells were treated with rLTGF-β1 and/or KTFR for 24h to show that
316 KTFR inhibits LTGF-β1 auto-activation. This could be demonstrated by the SEAP assay
317 **(Figure 4H)**. Furthermore, KTFR pre-treatment inhibited TSP-1-, ADAMTS1-, MMP-2-, and
318 MMP-9-mediated rLTGF-β1 activation **(Figure 4I)**. In addition, treatment of LX-2 HSCs
319 with KTFR reduced siECM1-induced active TGF-β1 levels, as evident from mRNA
320 expression of *ACTA2*, *COL1A1*, *COL3A1*, and *TIMP1* **(Figure 4J)**, protein levels of COL3A1
321 and TIMP1 **(Figure 4K)**, and IF staining of TGF-β1 LAP-D R58 **(Figure 4L)**.
322 MMPs mediate LTGF-β1 activation by proteolytic cleavage of LAP [27]. To investigate
323 whether ECM1 affects the proteolytic activity of MMP-2 or MMP-9, we performed
324 fluorogenic MMP activity assays. Incubation of MMP-2 or MMP-9 with rECM1 at a ratio of
325 1:2 (20ng MMP-2 or -9 and 40ng rECM1) inhibited the proteolytic activity of MMP-2 and
326 MMP-9 **(Figure 4M)**.
327 In summary, we show that the abrogative effect of ECM1 on LTGF-β1 activation by TSP-1 or
328 ADAMTS1 integrates at the KRFK or KTFR amino acid sequence. Additionally, ECM1
329 binds to mature MMP-2 and MMP-9 and thereby inhibits their proteolytic activity, thus
330 reducing LAP degradation and LTGF-β1 activation.

331 **Overexpression of ECM1 inhibits KRFK-induced LTGF-β1 activation in murine livers**
332 Since a KRFK peptide challenge phenocopied TSP-1's function regarding LTGF-β1
333 activation, we expected that treatment of mice with the KRFK peptide would lead to higher
334 levels of active TGF-β1 and increased fibrogenesis. To test whether ECM1 can prevent
335 KRFK-induced LTGF-β1 activation *in vivo* and thus rescue any resulting liver injury, we
336 treated 8-weeks-old WT mice with control or AAV8-ECM1 for 7 days prior to daily
337 intraperitoneal injections of 100 µg KRFK or KQFK (negative control) peptide for 14
338 consecutive days **(Figure 5A)**. The KRFK injections caused a significant upregulation of
339 HSC-specific fibrosis markers such as *Acta2*/α-SMA **(Figure 5B-D)** and collagen types
340 *Col1α1* and *Col3α1* **(Figure 5B)** all of which were also upregulated in 2- and 5-weeks-old
341 *Ecm1*-KO mice **(Figure 1I)**. Further, IHC staining of TGF-β1 LAP-D R58, H&E, and
342 picrosirius red (PSR) staining demonstrated that KRFK peptide treatment caused significant
343 LTGF-β1 activation and hepatocyte injury as displayed by cleared-out cytoplasm, and
344 pericentral liver fibrosis **(Figure 5E)**. Cell apoptosis was assessed by IHC staining of cleaved
345 caspase 3 to further investigate the type of KRFK-mediated liver injuries, however, we did

346 not detect increased hepatocyte apoptosis compared to the control group (**Figure S5A**). This
347 suggests that KRFK treatment is sufficient to induce mild fibrosis, however is not sufficient
348 for hepatocyte apoptosis levels. In turn, prior AAV8-mediated overexpression of ECM1
349 prevented the pro-fibrogenic changes induced by the KRFK peptide, as evident from reduced
350 levels of *Acta2*/α-SMA **(Figure 5B-D)**, decreased mRNA expression of fibrillar collagens
351 type *Col1α1* and *Col3α1* **(Figure 5B)**, and less detection of TGF-β1 LAP-D R58 **(Figure 5E)**.
352 Further, AAV8-ECM1 pre-treated mice presented with less evidence of liver injury in H&E
353 staining and fewer areas of fibrosis on PSR staining. Taken together, ECM1 overexpression
354 effectively prevents liver injury and fibrosis caused by KRFK-mediated activation of LTGF-
355 β1, suggesting a potential benefit in TSP-1-driven disease settings [34].

356 **KTFR reverses *Ecm1*-KO-induced liver injury in mice**

357 As KTFR suppressed LTGF-β1 activation *in vitro* **(Figure 4H-L)**, we injected 100 μg KTFR
358 peptide into 8-weeks-old *Ecm1*-KO mice for 14 consecutive days to test if we could
359 ameliorate the LTGF-β1 activation causing progressive liver injury in *Ecm1*-KO mice
360 **(Figure 6A)**. A KQFK peptide was used as a negative control. Surprisingly, KTFR treatment
361 was able to revert the *Ecm1*-KO phenotype. RT-qPCR and immunoblotting data showed that
362 fibrosis markers in *Ecm1*-KO livers were attenuated by KTFR peptide injections, including
363 *Col1α1*, *Col3α1*, *Timp1*, and *Acta2*/α-SMA **(Figure 6B, C)**. IF or IHC staining of α-SMA and
364 TGF-β1 LAP-D (R58) further confirmed the inhibitory effect of KTFR on *Ecm1*-KO-
365 mediated HSC and LTGF-β1 activation **(Figure 6D, E)**. H&E and PSR stainings exhibited
366 perisinusoidal fibrosis in *Ecm1*-KO mice as shown by extracellular matrix deposition being
367 attenuated by KTFR peptide injection **(Figure 6E)**. In addition, 10-week-old *Ecm1*-KO mice
368 exhibited cell apoptosis in a few hepatocytes, characterized by nuclear expression of cleaved
369 caspase 3 and cell shrinkage compared to WT mice, which was alleviated by KTFR treatment
370 (**Figure S5B**, indicated by arrows).
371 *In vivo*, KTFR peptide exerts an effect similar to that of ECM1 and reverts the liver injury
372 suffered by mice upon *Ecm1*-KO at 8 weeks of age and could serve to restore ECM1's
373 functions where lost.

374 **KTFR alleviates liver injury in *Fxr*-KO mice.**

375 Farnesoid X receptor (FXR, NR1H4) plays fundamental roles in maintaining bile acid
376 homeostaisis, modulating metabolism, and reducing inflammation [35]. *Fxr*-KO mice are
377 characterized by cholestatic liver injury, HSC activation, fibrosis, and subsequcently

378 progression to HCC [35, 36]. We observed that the expression of *Ecm1* was significantly
379 decreased in *Fxr*-KO mice while TGF-β1 mRNA expression remained unaffected (**Figure**
380 **S6A**), which suggested that fibrosis in *Fxr*-KO mice was primarily due to LTGF-β1 activation.
381 In consequence, *Fxr*-KO mouse model may represent an ideal platform for further validation
382 and asessment of the anti-fibrotic potential of the KTFR peptide. Therefore, 100 μg KTFR or
383 KQFK (negative control) peptide were injected into 8-week-old *Fxr*-KO mice for 14
384 consecutive days (**Figure 7A**). RT-qPCR and immunoblotting analyses demonstrated that the
385 increased fibrosis markers in *Fxr*-KO livers, including *Col1α1*, *Col3α1*, *Timp1*, and *Acta2*,
386 were rescued following KTFR peptide treatment **(Figure 7B, C)**. IF or IHC staining of α-
387 SMA and TGF-β1 LAP-D (R58) further confirmed the inhibitory effect of KTFR on HSC and
388 LTGF-β1 activation in *Fxr*-KO mice **(Figure 7D, E)**. H&E and PSR stainings revealed
389 pericentral fibrosis in *Fxr*-KO mice, characterized by extracellular matrix deposition around
390 the central veins, which was attenuated by KTFR peptide injection **(Figure 7E)**. Similar to
391 *Ecm1*-KO mice, mild hepatocyte apoptosis induced by *Fxr*-KO was prevented by KTFR
392 treatment, as assessed by IHC staining of cleaved caspase 3 (**Figure S6B**, indicated by
393 arrows). These results confirmed the anti-fibrotic effect of KTFR in *Fxr*-KO mice.

394 **ECM1 loss correlates with upregulated mediators of LTGF-β1 activation in CLD**

395 To investigate the relationship between ECM1 downregulation and LTGF-β1 activation in
396 patients, we performed RNAscope, IF or IHC staining for ECM1, TGF-β1 LAP-D (R58),
397 TSP-1, ADAMTS1, MMP-2 and MMP-9 in paraffin-embedded tissue samples from patients
398 suffering from either F1-F2 liver fibrosis (n=6) or ALD-/HBV-induced liver cirrhosis (n=15)
399 and compared those to relatively healthy individuals (n=5). In parallel with the progressive
400 decrease of ECM1 expression on RNA and protein level **(Figure 8A, B)**, TGF-β1 LAP-D
401 (R58) staining intensity increased from control to F1-2 stage fibrosis and on to cirrhosis
402 **(Figure 8C)** indicating a significant and inverse correlation. Interestingly, expression of the
403 tested LTGF-β1 activators, TSP-1, ADAMTS1, MMP-2 and MMP-9 increased consistently
404 with progressing liver fibrosis **(Figure 8C)**. This suggests that in parallel with ECM1
405 downregulation, the bioavailability of the mediators increase as well in order to provide active
406 TGF-β1 for surrounding liver tissue in its response to damage. This was further confirmed
407 across different etiologies of liver injury by analysing the GEO DataSets (GSE49541) that
408 comprises RNAseq data of liver tissue from NAFLD patients with mild (n=40) or advanced
409 (n=32) fibrosis [37]. ECM1 expression decreased with disease severity, while mRNA levels
410 of LTGF-β1 activators increased including that of *TSP-1*, *TSP-2*, *ADAMTS1*, *ADAMTS2*,

411 *MMP-2*, *MMP-9*, *ITGAV*, and *ITGB1*. As this would lead to enhanced availability of active
412 TGF-β1, downstream activation of HSCs can be expected, which was supported by increased
413 expression levels of fibrotic collagens, such as *COL1A1*, *COL1A2*, *COL3A1*, and *COL4A1* in
414 cohorts with more advanced fibrosis **(Figure 8D)**. Additionally, we analyzed human single
415 cell (sc)RNAseq (GSE174748) of liver tissue from normal and NAFLD cirrhotic samples [7].
416 After quality filtering, 30,918 cells, with an average sequencing depth of 2,000 genes per cell,
417 were subjected to further analysis. Unsupervised clustering classified these cells into 14
418 different clusters **(Figure S7A)**, and Cluster 10 was defined as HSCs based on the expression
419 of HSC-specific marker genes **(Figure S7B)**. Uniform manifold approximation and projection
420 (UMAP) visualization showed that HSCs could be divided into two clusters: quiescent HSCs
421 (qHSCs) and active HSCs (aHSCs) **(Figure S7C, 8E)**. With *ECM1* was abundant in
422 quiescent HSCs, LTGF-β1 activators (*TSP-1*, *ADAMTS1*, *MMP-2*, *MMP-9*), and fibrotic
423 markers (*ACTA2*, *COL1A1*) were highly enriched in activated HSCs (**Figure 8F, G**). In
424 consequence, we hypothesize that the sequence of events in CLD expression starts with
425 ECM1 downregulation and upregulation of LTGF-β1 activators, followed by LTGF-β1 and
426 HSC activation and finally, increased extracellular matrix production and deposition **(Figure**
427 **9A, B)**.

428 **Compartment modeling confirms consistency of effects of ECM1 on the liver fibrosis**
429 **interaction network**

430 In order to verify the experimentally observed behavior of ECM1, we established a
431 computational model that represents the key network of cellular phenotypes and their
432 hypothesized interactions **(Figure S8)**. To simulate the process of fibrogenesis, we ran the
433 simulation for 21 days which represents 6 injections of CCl_4 (at days 1, 4, 8, 11, 15 and 18,
434 following the experimental administration scheme) under four different ECM1 production
435 rates as shown in Figure 9C. The first dose of CCl_4 was injected at day 1, when the
436 equilibrium was reached. The overall temporal dynamics of the displayed network
437 components well reproduced the known or expected behavior of chronic liver injury. When
438 the production rate of ECM1 was increased in the simulation, the amount of E-Protease
439 (degrades ECM1 in our model), L-Mediator (activates LTGF-β1 in our model) and active
440 TGF-β1 decreased. The quantity of aHSC and fibrotic collagen dropped as the production rate
441 of ECM1 increased. The mass of hepatocytes and macrophages in the compartment, however,
442 was not influenced, even though the small dispersion of the curves for hepatocytes at 20 days
443 indicates that in case of even higher fibrotic collagen concentrations, the hepatocyte mass may

444 be affected by ECM1 production **(Figure 9C)**. In summary, when incorporating the role of
445 ECM1 as delineated in our experiments, the compartment model accurately describes
446 development and progression of hepatic fibrosis following chronic liver injury. The reduced
447 levels of ECM1 lead to increased production of fibrotic matrix. This supports the
448 experimental conclusion that ECM1 represents a suitable therapeutic target to reverse hepatic
449 fibrosis.

450 **Discussion**

451 The present study shows that ECM1 inhibits LTGF-β1 activation mediated by TSP-1,
452 ADAMTS1, MMP-2 and MMP-9 and thus attenuates hepatic fibrosis **(Figure 9A, B)**. TSP-1
453 and ADAMTS1 cause a conformational change within LAP of the LTGF-β1 complex, through
454 their respective KRFK or KTFR motifs binding to LAP's LSKL sequence, thereby releasing
455 the active cytokine [32, 38, 39]. Interestingly, while the KRFK peptide can independently
456 activate LTGF-β1**(Figure S9A, B)**, KTFR exposure requires collaboration with another motif
457 within ADAMTS1 to release the active TGF-β1 **(Figure S9C, D)**. Thus, the presence of a
458 KTFR peptide alone suffices to maintain the integrity of LTGF-β1, not allowing its activation.
459 In contrast, MMP-2 and MMP-9 act via proteolytical cleavage of LAP, resulting in LTGF-β1
460 activation [27]. It has been shown that the C-terminal tandem repeat 2 (amino acids 236-361)
461 of ECM1 binds to MMP-9 thus reducing its activity [40]. Whether this C-terminal repeat or
462 any other sequence of ECM1 interacts with MMP-2 needs further investigation.

463 To further verify our findings in liver tissue of patients suffering from CLD, we show that
464 with ECM1 downregulation and LTGF-β1 activation, there is a significantly increased
465 expression of LTGF-β1 activating mediators, including TSP-1, ADAMTS1, MMP-2, and
466 MMP-9 which correlate with the progressing fibrosis **(Figure 8A-C)**. It is known that
467 activated HSCs and injured hepatocytes are the major source for TSP-1 [41], ADAMTS1
468 [42], as well as MMP-2 and MMP-9 [43] in fibrotic liver disease, indicating that expression
469 levels of LTGF-β1 activators are useful parameters to predict liver damage. It remains a
470 challenge to directly investigate the activity of TSP-1, ADAMTS1, MMP-2, and MMP-9 in
471 patient liver tissue, but we were able to show their activity indirectly by staining for TGF-β1
472 LAP-D R58.

473 To delve deeper into the impact of these mediators on TGF-β1 activation, we examined the
474 mRNA expression of TGF-β1 in LX-2 HSCs treated with control or αvβ6 integrin/TSP-
475 1/ADAMTS1/MMP-2/MMP-9 and found an induction of TGF-β1 mRNA expression **(Figure**
476 **S10A)**. Whether it stems from TGF-β1's positive and self-sustained feedback loop on its own

477 expression or from LTGF-β1 activators facilitating TGF-β1 transcription remains
478 inadequately explored and warrants further study. We hypothesize that reverting the loss of
479 ECM1 might disrupt the observed self-perpetuating circle of TGF-β1 activation and
480 expression. Reversely, we also investigated whether ECM1 affected the expression of its
481 activators. ECM1 overexpression inhibited the mRNA expression of αvβ6 integrin, TSP-1,
482 ADAMTS1, MMP-2, and MMP-9, while rECM1 did not significantly reduce their
483 expressions (**Figure S10B, C**). These findings in combination with our interaction studies and
484 SEAP assays (**Figure 3, 4**) suggest that ECM1 does indeed inhibit mediator-induced LTGF-
485 β1 activation, but it may also attenuate liver fibrosis by preventing their expression. It is
486 currently not clear how ECM1 could control the expression of TSP-1/ADAMTS1/MMP-
487 2/MMP-9 beyond TGF-β1 bioavailability. Additionally, we investigated the effects of ECM1
488 on HSC behavior by ECM1 overexpression or knockdown in LX-2 cells. ECM1
489 overexpression significantly inhibited cell proliferation (**Figure S11A-C**) and migration
490 (**Figure S11D**), while ECM1 knockdown did not affect proliferation (**Figure S11E-G**) but
491 appeared to promote cell migration (**Figure S11H**). As LX-2 cells are activated HSCs with a
492 comparatively low level of ECM1 expression versus quiescent HSCs, further analyses with
493 ECM1 knockdown should be conducted in primary HSCs to provide more relevant insights.
494 ECM1 is predominantly expressed by hepatocytes and to a lesser extent by quiescent HSCs,
495 which secrete it into the liver's extracellular matrix, to protect the matrix-deposited LTGF-β1
496 from activation by the mediators and subsequent fibrogenic signaling. In addition to HSCs
497 and TGF-β1, CLD progression involves a plethora of cell types and signals. Therefore, we
498 used computational modelling to further investigate the hepatoprotective effect of ECM1
499 **(Figure 9C)**. The simulated temporal dynamics of the proposed *in silico* model predict that
500 indeed ECM1 availability might be a limiting factor that can be overcome to attenuate injury
501 in CLD. Extending this network in the future and resolving it in space and time, as recently
502 demonstrated for liver regeneration [44], will inform a future multi-scale model, or a digital
503 liver twin. Precise *in silico* modelling will allow researchers to predict the impact of the up- or
504 down-regulation of each element on all other network components and could lead to a better
505 understanding of the entire disease process, and help us anticipate the possible success of
506 future therapeutic interventions.
507 Reliable and safe delivery to the human liver is essential for antifibrotic treatment. It may be
508 possible to employ recombinant proteins or phenocopying peptides [45], viral vectors such as
509 adeno-associated viruses (AAV), which have already been employed in gene therapy [46],
510 bacterial delivery [47] methods to restore ECM1 expression or function in diseased livers.

Short synthetic peptides are a promising strategy, as they have been successfully employed in the treatment of multiple sclerosis and NASH [48, 49]. Therefore, a peptide sequence of the ECM1 protein that confers its function on LTGF-β1 bioavailability and prevents it from excessive activation or a direct application of the KFTR peptide as shown experimentally *in vivo* might provide a liver-specific, anti-fibrotic intervention, which are still not available at the present time [49, 50].

Materials and Methods

Human samples, mouse experiments, chemical reagents, primers, antibodies used in this study, and further detailed information on the methods are presented in the supplementary materials.

References and Notes

1 Hagstrom H, Nasr P, Ekstedt M, Hammar U, Stal P, Hultcrantz R*, et al.* Fibrosis stage but not NASH predicts mortality and time to development of severe liver disease in biopsy-proven NAFLD. J Hepatol 2017;**67**:1265-73.

2 Sanyal AJ. Past, present and future perspectives in nonalcoholic fatty liver disease. Nat Rev Gastroenterol Hepatol 2019;**16**:377-86.

3 Mathieu E, Meheus L, Raymackers J, Merregaert J. Characterization of the osteogenic stromal cell line MN7: identification of secreted MN7 proteins using two-dimensional polyacrylamide gel electrophoresis, western blotting, and microsequencing. J Bone Miner Res 1994;**9**:903-13.

4 Smits P, Poumay Y, Karperien M, Tylzanowski P, Wauters J, Huylebroeck D*, et al.* Differentiation-dependent alternative splicing and expression of the extracellular matrix protein 1 gene in human keratinocytes. J Invest Dermatol 2000;**114**:718-24.

5 Chan I. The role of extracellular matrix protein 1 in human skin. Clin Exp Dermatol 2004;**29**:52-6.

6 Fan W, Liu T, Chen W, Hammad S, Longerich T, Hausser I*, et al.* ECM1 Prevents Activation of Transforming Growth Factor beta, Hepatic Stellate Cells, and Fibrogenesis in Mice. Gastroenterology 2019;**157**:1352-67 e13.

7 Filliol A, Saito Y, Nair A, Dapito DH, Yu LX, Ravichandra A*, et al.* Opposing roles of hepatic stellate cell subpopulations in hepatocarcinogenesis. Nature 2022;**610**:356-65.

8 Colak S, Ten Dijke P. Targeting TGF-beta Signaling in Cancer. Trends Cancer 2017;**3**:56-71.

9 Fabregat I, Moreno-Caceres J, Sanchez A, Dooley S, Dewidar B, Giannelli G*, et al.* TGF-beta signalling and liver disease. FEBS J 2016;**283**:2219-32.

10 Yang Z, Mu Z, Dabovic B, Jurukovski V, Yu D, Sung J*, et al.* Absence of integrin-mediated TGFbeta1 activation in vivo recapitulates the phenotype of TGFbeta1-null mice. J Cell Biol 2007;**176**:787-93.

11 Elliott RL, Blobe GC. Role of transforming growth factor Beta in human cancer. J Clin Oncol 2005;**23**:2078-93.

12 Dooley S, ten Dijke P. TGF-β in progression of liver disease. Cell Tissue Res 2012;**347**:245-56.

551 13 Dewidar B, Meyer C, Dooley S, Meindl-Beinker AN. TGF-β in Hepatic Stellate Cell
552 Activation and Liver Fibrogenesis-Updated 2019. Cells 2019;**8**.
553 14 Robertson IB, Rifkin DB. Regulation of the Bioavailability of TGF-β and TGF-β-Related
554 Proteins. Cold Spring Harb Perspect Biol 2016;**8**.
555 15 Li Y, Fan W, Link F, Wang S, Dooley S. Transforming growth factor β latency: A
556 mechanism of cytokine storage and signalling regulation in liver homeostasis and disease.
557 JHEP Rep 2022;**4**:100397.
558 16 Dong X, Zhao B, Iacob RE, Zhu J, Koksal AC, Lu C*, et al.* Force interacts with
559 macromolecular structure in activation of TGF-β. Nature 2017;**542**:55-9.
560 17 Wipff PJ, Rifkin DB, Meister JJ, Hinz B. Myofibroblast contraction activates latent TGF-
561 beta1 from the extracellular matrix. J Cell Biol 2007;**179**:1311-23.
562 18 Jenkins G. The role of proteases in transforming growth factor-beta activation. Int J
563 Biochem Cell Biol 2008;**40**:1068-78.
564 19 Barcellos-Hoff MH, Dix TA. Redox-mediated activation of latent transforming growth
565 factor-beta 1. Mol Endocrinol 1996;**10**:1077-83.
566 20 Shi M, Zhu J, Wang R, Chen X, Mi L, Walz T*, et al.* Latent TGF-β structure and
567 activation. Nature 2011;**474**:343-9.
568 21 Brown PD, Wakefield LM, Levinson AD, Sporn MB. Physicochemical activation of
569 recombinant latent transforming growth factor-beta's 1, 2, and 3. Growth Factors 1990;**3**:35-
570 43.
571 22 Wang H, Kochevar IE. Involvement of UVB-induced reactive oxygen species in TGF-
572 beta biosynthesis and activation in keratinocytes. Free Radic Biol Med 2005;**38**:890-7.
573 23 Breitkopf K, Godoy P, Ciuclan L, Singer MV, Dooley S. TGF-beta/Smad signaling in the
574 injured liver. Z Gastroenterol 2006;**44**:57-66.
575 24 Castilla A, Prieto J, Fausto N. Transforming growth factors beta 1 and alpha in chronic
576 liver disease. Effects of interferon alfa therapy. N Engl J Med 1991;**324**:933-40.
577 25 Schultz-Cherry S, Murphy-Ullrich JE. Thrombospondin causes activation of latent
578 transforming growth factor-beta secreted by endothelial cells by a novel mechanism. J Cell
579 Biol 1993;**122**:923-32.
580 26 Bourd-Boittin K, Bonnier D, Leyme A, Mari B, Tuffery P, Samson M*, et al.* Protease
581 profiling of liver fibrosis reveals the ADAM metallopeptidase with thrombospondin type 1
582 motif, 1 as a central activator of transforming growth factor beta. Hepatology 2011;**54**:2173-
583 84.
584 27 Yu Q, Stamenkovic I. Cell surface-localized matrix metalloproteinase-9 proteolytically
585 activates TGF-beta and promotes tumor invasion and angiogenesis. Genes Dev 2000;**14**:163-
586 76.
587 28 He L, Yuan H, Liang J, Hong J, Qu C. Expression of hepatic stellate cell activation-
588 related genes in HBV-, HCV-, and nonalcoholic fatty liver disease-associated fibrosis. PloS
589 one 2020;**15**:e0233702.
590 29 Weiskirchen R, Weimer J, Meurer SK, Kron A, Seipel B, Vater I*, et al.* Genetic
591 characteristics of the human hepatic stellate cell line LX-2. PLoS One 2013;**8**:e75692.
592 30 Gressner AM, Weiskirchen R, Breitkopf K, Dooley S. Roles of TGF-beta in hepatic
593 fibrosis. Front Biosci 2002;**7**:d793-807.
594 31 Abramson J, Adler J, Dunger J, Evans R, Green T, Pritzel A*, et al.* Accurate structure
595 prediction of biomolecular interactions with AlphaFold 3. Nature 2024.
596 32 Schultz-Cherry S, Chen H, Mosher DF, Misenheimer TM, Krutzsch HC, Roberts DD*, et*
597 *al.* Regulation of transforming growth factor-beta activation by discrete sequences of
598 thrombospondin 1. J Biol Chem 1995;**270**:7304-10.

599 33 Laurent MA, Bonnier D, Théret N, Tufféry P, Moroy G. In silico characterization of the
600 interaction between LSKL peptide, a LAP-TGF-beta derived peptide, and ADAMTS1. Comput
601 Biol Chem 2016;**61**:155-61.
602 34 Li Y, Turpin CP, Wang S. Role of thrombospondin 1 in liver diseases. Hepatol Res
603 2017;**47**:186-93.
604 35 Zhou J, Cui S, He Q, Guo Y, Pan X, Zhang P*, et al.* SUMOylation inhibitors synergize
605 with FXR agonists in combating liver fibrosis. Nat Commun 2020;**11**:240.
606 36 Wolfe A, Thomas A, Edwards G, Jaseja R, Guo GL, Apte U. Increased activation of the
607 Wnt/beta-catenin pathway in spontaneous hepatocellular carcinoma observed in farnesoid
608 X receptor knockout mice. J Pharmacol Exp Ther 2011;**338**:12-21.
609 37 Moylan CA, Pang H, Dellinger A, Suzuki A, Garrett ME, Guy CD*, et al.* Hepatic gene
610 expression profiles differentiate presymptomatic patients with mild versus severe
611 nonalcoholic fatty liver disease. Hepatology 2014;**59**:471-82.
612 38 Young GD, Murphy-Ullrich JE. The tryptophan-rich motifs of the thrombospondin
613 type 1 repeats bind VLAL motifs in the latent transforming growth factor-beta complex. J Biol
614 Chem 2004;**279**:47633-42.
615 39 Soriano-Romani L, Contreras-Ruiz L, Lopez-Garcia A, Diebold Y, Masli S. Topical
616 Application of TGF-beta-Activating Peptide, KRFK, Prevents Inflammatory Manifestations in
617 the TSP-1-Deficient Mouse Model of Chronic Ocular Inflammation. International journal of
618 molecular sciences 2018;**20**.
619 40 Fujimoto N, Terlizzi J, Aho S, Brittingham R, Fertala A, Oyama N*, et al.* Extracellular
620 matrix protein 1 inhibits the activity of matrix metalloproteinase 9 through high-affinity
621 protein/protein interactions. Exp Dermatol 2006;**15**:300-7.
622 41 El-Youssef M, Mu Y, Huang L, Stellmach V, Crawford SE. Increased expression of
623 transforming growth factor-beta1 and thrombospondin-1 in congenital hepatic fibrosis:
624 possible role of the hepatic stellate cell. J Pediatr Gastroenterol Nutr 1999;**28**:386-92.
625 42 Schwettmann L, Wehmeier M, Jokovic D, Aleksandrova K, Brand K, Manns MP*, et al.*
626 Hepatic expression of A disintegrin and metalloproteinase (ADAM) and ADAMs with
627 thrombospondin motives (ADAM-TS) enzymes in patients with chronic liver diseases. J
628 Hepatol 2008;**49**:243-50.
629 43 Roderfeld M. Matrix metalloproteinase functions in hepatic injury and fibrosis. Matrix
630 Biol 2018;**68-69**:452-62.
631 44 Jieling Zhao AG, Reham Hassan, Steven Dooley, Jan Georg Hengstler, Dirk Drasdo A
632 liver digital twin for in silico testing of cellular and inter-cellular mechanisms in regeneration
633 after drug-induced damage. iScience 2023.
634 45 Apostolopoulos V, Bojarska J, Chai TT, Elnagdy S, Kaczmarek K, Matsoukas J*, et al.* A
635 Global Review on Short Peptides: Frontiers and Perspectives. Molecules 2021;**26**.
636 46 George LA, Monahan PE, Eyster ME, Sullivan SK, Ragni MV, Croteau SE*, et al.*
637 Multiyear Factor VIII Expression after AAV Gene Transfer for Hemophilia A. N Engl J Med
638 2021;**385**:1961-73.
639 47 Kreitz J, Friedrich MJ, Guru A, Lash B, Saito M, Macrae RK*, et al.* Programmable
640 protein delivery with a bacterial contractile injection system. Nature 2023;**616**:357-64.
641 48 La Mantia L, Munari LM, Lovati R. Glatiramer acetate for multiple sclerosis. Cochrane
642 Database Syst Rev 2010:Cd004678.
643 49 Wai-Sun Wong V, Anstee QM, Nitze LM, Geerts A, George J, Nolasco V*, et al.*
644 FibroScan-aspartate aminotransferase (FAST) score for monitoring histological improvement
645 in non-alcoholic steatohepatitis activity during semaglutide treatment: post-hoc analysis of a

646 randomised, double-blind, placebo-controlled, phase 2b trial. EClinicalMedicine
647 2023;**66**:102310.
648 50 Harrison SA, Wong VW, Okanoue T, Bzowej N, Vuppalanchi R, Younes Z*, et al.*
649 Selonsertib for patients with bridging fibrosis or compensated cirrhosis due to NASH: Results
650 from randomized phase III STELLAR trials. J Hepatol 2020;**73**:26-39.

651 **Figures legends**

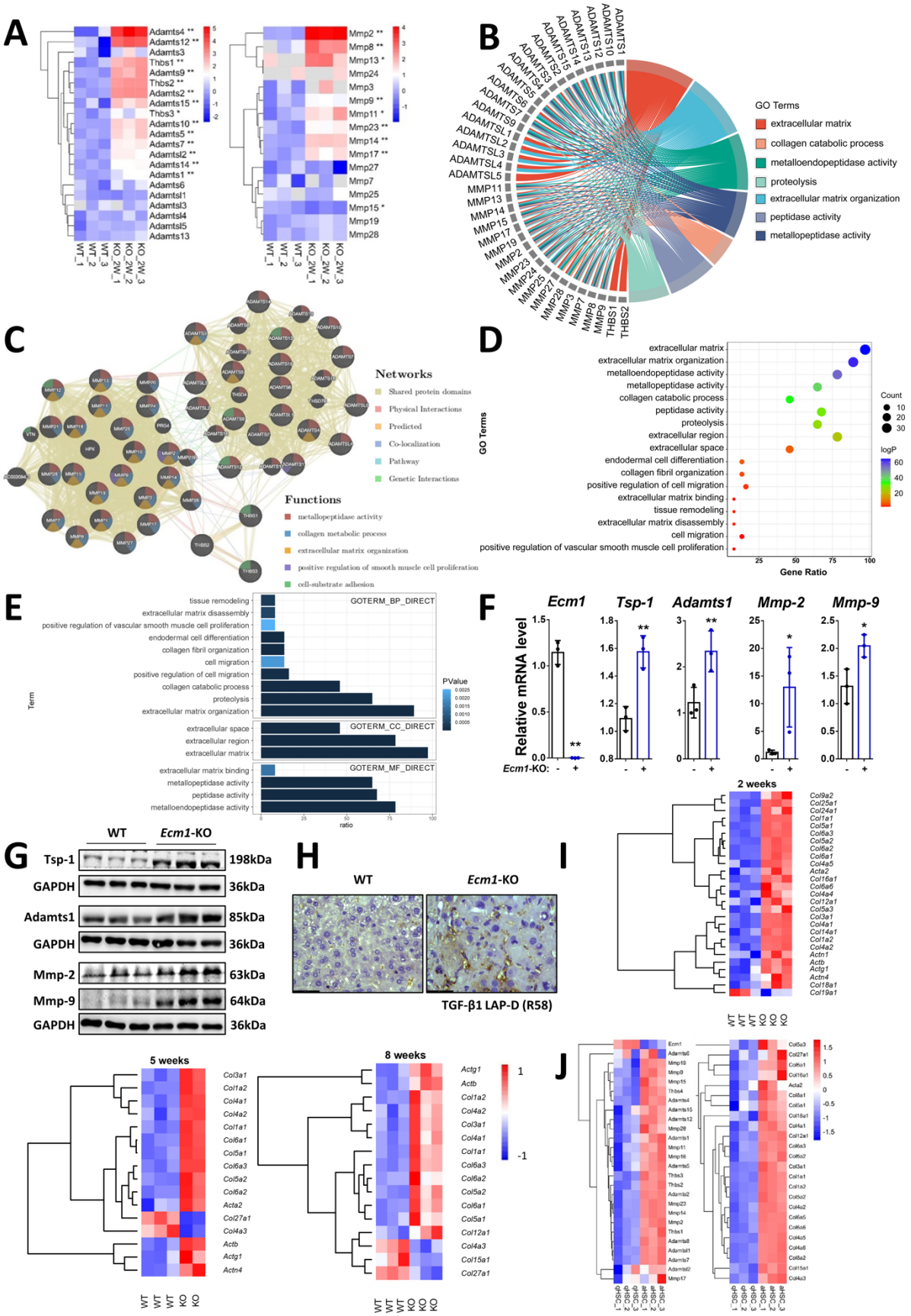

652 **Figure 1. ECM1 depletion causes the upregulation of mediators of LTGF-β activation**
653 **and severe fibrogenesis in liver.**
654 **(A)** RNAseq analysis of the expression of *Mmps*, *Tsps*, and *Adamtss* in 2 weeks old *Ecm1*-KO
655 as compared to *WT* mice. **(B)** Chord diagram, illustrating the main biological processes the
656 upregulated proteases are involved in. **(C)** Interconnectivity of the upregulated MMps, Tsps,
657 and Adamtss. **(D, E)** GO pathways influenced by *Ecm1*-KO-induced proteases. **(F, G)**
658 Relative mRNA and protein levels of Tsp-1, Adamts1, Mmp-2, and Mmp-9 in liver tissue
659 from WT and *Ecm1*-KO mice. **(H)** Representative images of IHC stainings for TGF-β1 LAP-
660 D (R58) in liver tissue from *Ecm1*-KO and *WT* mice. Scale bar, 43.5 μm. **(I)** RNA-Seq
661 analysis, demonstrating the upregulation of fibrotic genes in *Ecm1*-KO mice at the age of 2, 5
662 and 8 weeks. **(J)** mRNA expression of *Ecm1*, LTGF-β1 activators, and fibrotic markers in
663 quiescent and activated HSCs isolated from control or CCl_4-treated mice (n=3), extracted
664 from GEO DataSets GSE149508. For RT-qPCR, human *PPIA* was used as an endogenous
665 control. For Western blotting, GAPDH was used as a loading control. P-values were
666 calculated by unpaired Student's t-test. Bars represent mean ± SD. *$p<0.05$; **$p<0.01$.

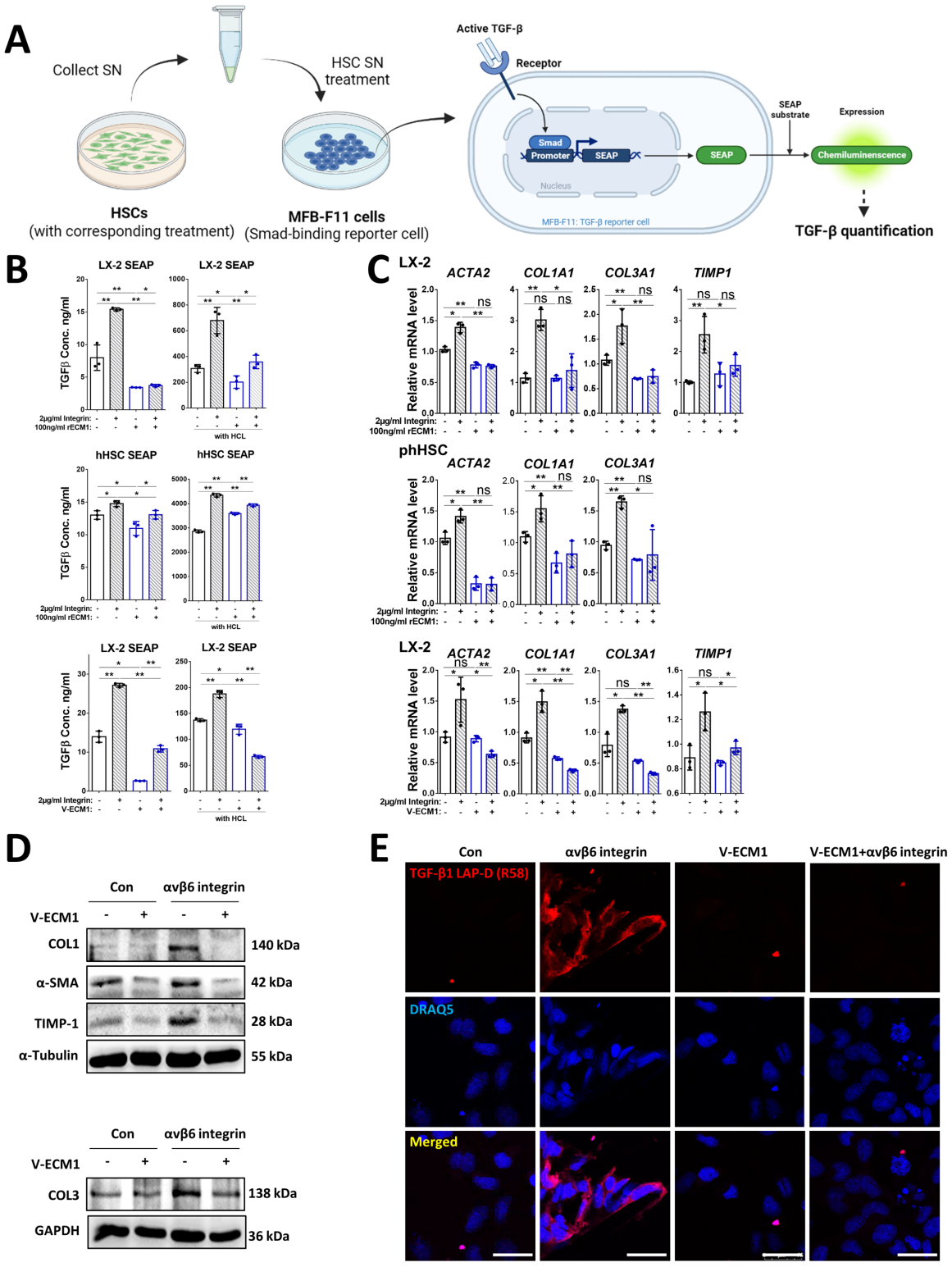
A
Collect SN
HSC SN treatment
Active TGF-β
Receptor
Smad
Promoter
SEAP
SEAP
SEAP substrate
Expression
Chemiluminenscence
Nucleus
MFB-F11: TGF-β reporter cell
HSCs
(with corresponding treatment)
MFB-F11 cells
(Smad-binding reporter cell)
TGF-β quantification
B
LX-2 SEAP
hHSC SEAP
TGFβ Conc. ng/ml
2μg/ml Integrin:
100ng/ml rECM1:
V-ECM1:
with HCL
C
LX-2
phHSC
ACTA2
COL1A1
COL3A1
TIMP1
Relative mRNA level
ns
D
Con
αvβ6 integrin
V-ECM1
COL1
α-SMA
TIMP-1
α-Tubulin
140 kDa
42 kDa
28 kDa
55 kDa
COL3
GAPDH
138 kDa
36 kDa
E
Con
αvβ6 integrin
V-ECM1
V-ECM1+αvβ6 integrin
TGF-β1 LAP-D (R58)
DRAQ5
Merged

667 **Figure 2. ECM1 inhibits αvβ6 integrin-mediated LTGF-β1 activation.**
668 **(A)** Illustration of SEAP activity assay used with the MFB-F11 TGF-β signaling reporter cell
669 line (Created with BioRender.com). **(B)** The concentration of active and total TGF-β (ng/ml)
670 measured by SEAP activity assay from conditioned LX-2 HSCs SN and phHSCs SN
671 incubated w/o rECM1/V-ECM1 and/or αvβ6 integrin. **(C)** Relative mRNA levels of *ACTA2,*
672 *COL1A1, COL3A1*, and *TIMP1* in LX-2 HSCs and phHSCs incubated w/o rECM1/V-ECM1
673 and/or αvβ6 integrin. **(D)** Protein levels of COL1, COL3, α-SMA, and TIMP1 in LX-2 HSCs
674 incubated with/without V-ECM1 and/or αvβ6 integrin. **(E)** Representative images of IF
675 stainings for TGF-β1 LAP-D (R58) in LX-2 HSCs incubated with/without V-ECM1 and/or
676 αvβ6 integrin. DRAQ5 was used for nuclear staining. Scale bar, 25 μm. For RT-qPCR, human
677 PPIA was used as an endogenous control. P-values were calculated by unpaired Student's t-
678 test. Bars represent mean ± SD. *$p<0.05$; **$p<0.01$. For Western blotting, GAPDH or α-
679 Tubulin were used as a loading control.

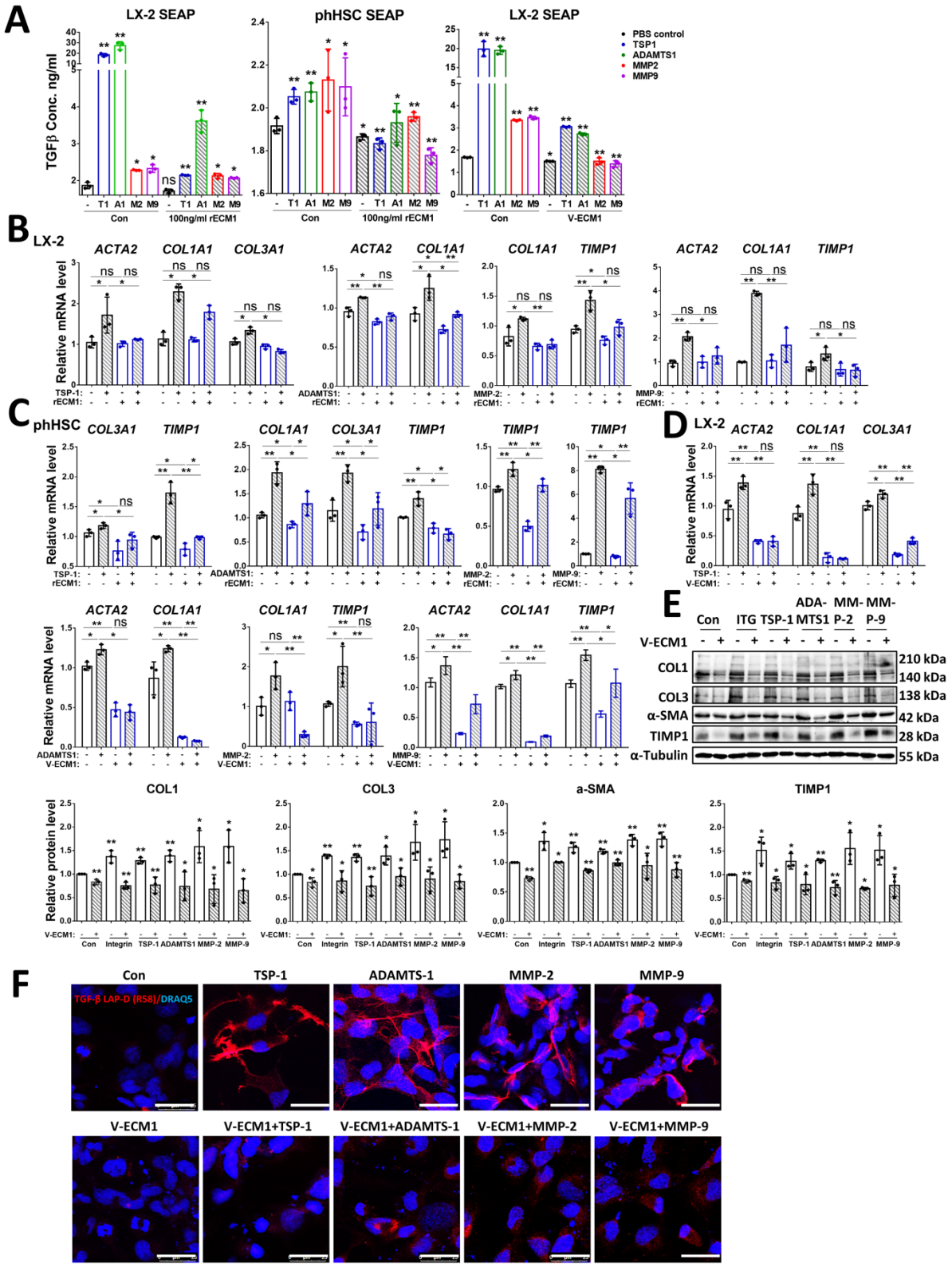
A
LX-2 SEAP
phHSC SEAP
LX-2 SEAP
TGFβ Conc. ng/ml
PBS control
TSP1
ADAMTS1
MMP2
MMP9
Con
100ng/ml rECM1
V-ECM1
B
LX-2
Relative mRNA level
ACTA2
COL1A1
COL3A1
TIMP1
C
phHSC
D
E
Con
ITG
TSP-1
ADA-MTS1
MM-P-2
MM-P-9
V-ECM1
COL1
COL3
α-SMA
TIMP1
α-Tubulin
210 kDa
140 kDa
138 kDa
42 kDa
28 kDa
55 kDa
Relative protein level
Integrin
F
Con
TSP-1
ADAMTS-1
MMP-2
MMP-9
TGF-β LAP-D (R58)/DRAQ5
V-ECM1
V-ECM1+TSP-1
V-ECM1+ADAMTS-1
V-ECM1+MMP-2
V-ECM1+MMP-9

680 **Figure 3. ECM1 inhibits TSP-1/ADAMTS1/MMP-2/MMP-9-mediated LTGF-β1**
681 **activation.**
682 **(A)** The concentration of active TGF-β (ng/ml) measured by SEAP activity assay from
683 conditioned LX-2 HSCs SN and phHSCs SN incubated w/o TSP-1/ADAMTS1/MMP-
684 2/MMP-9 and/or rECM1/V-ECM1. **(B-D)** Relative mRNA levels of *ACTA2, COL1A1*,
685 *COL3A1*, and *TIMP1* in LX-2 HSCs and phHSCs incubated with/without rECM1/V-ECM1
686 and/or TSP-1/ADAMTS1/MMP-2/MMP-9. **(E)** Protein levels of COL1, COL3, α-SMA, and
687 TIMP1 in LX-2 HSCs incubated with/without rECM1/V-ECM1 and/or Integrin, TSP-1,
688 ADAMTS1, MMP-2, or MMP-9. **(F)** Representative images of IF stainings for TGF-β1
689 LAP-D (R58) in LX-2 HSCs incubated with/without V-ECM1 and/or TSP-
690 1/ADAMTS1/MMP-2/MMP-9. DRAQ5 was used for nuclear staining. Scale bar, 25 μm. For
691 RT-qPCR, human PPIA was used as an endogenous control. P-values were calculated by
692 unpaired Student's t-test. Bars represent mean ± SD. *$p<0.05$; **$p<0.01$. For Western blotting,
693 α-Tubulin was used as a loading control. Quantification of protein expression was performed
694 using Image J (National Institute of Health, Bethesda, MD).

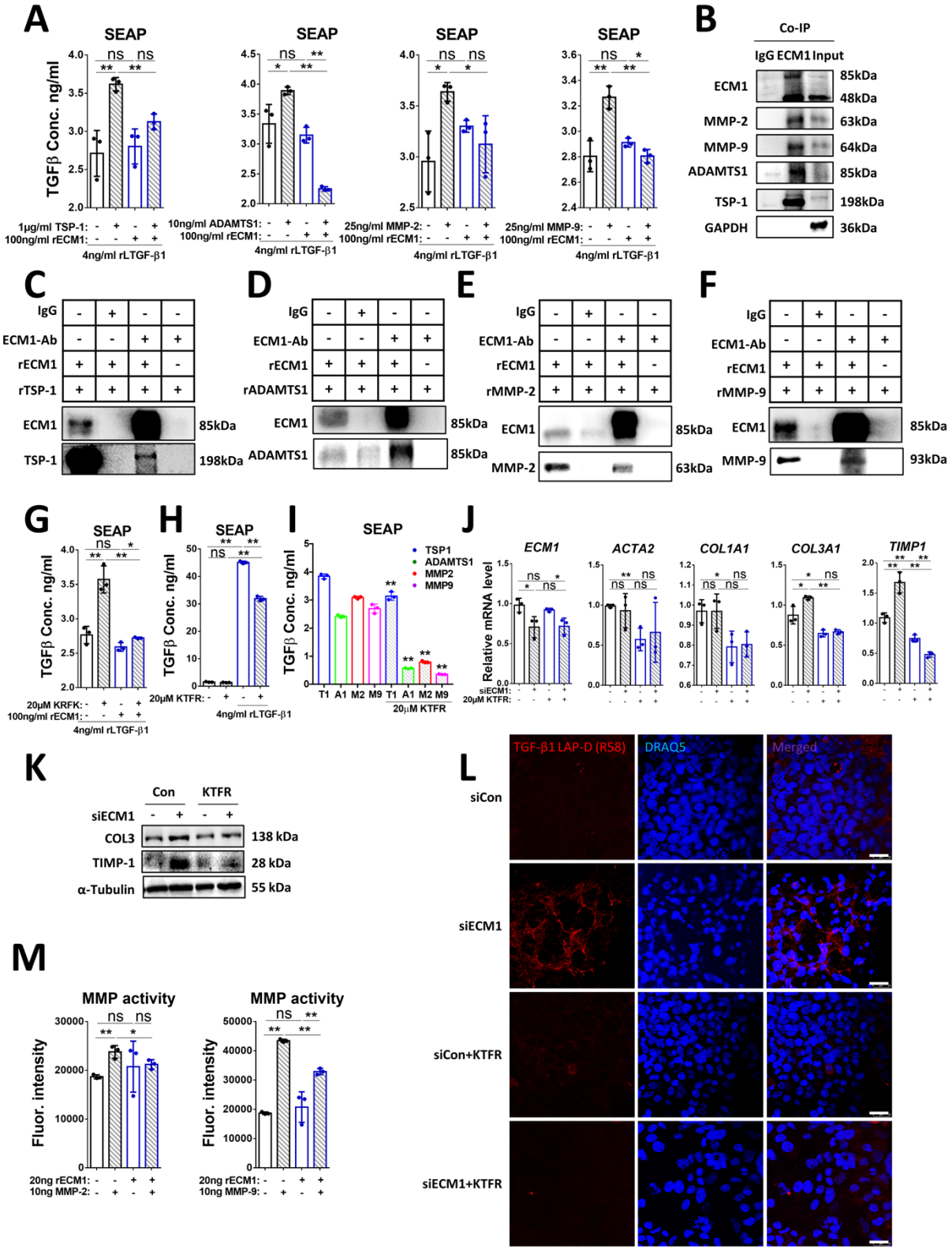
A
SEAP
TGFβ Conc. ng/ml
1μg/ml TSP-1:
100ng/ml rECM1:
4ng/ml rLTGF-β1
10ng/ml ADAMTS1:
25ng/ml MMP-2:
25ng/ml MMP-9:
B
Co-IP
IgG ECM1 Input
ECM1
MMP-2
MMP-9
ADAMTS1
TSP-1
GAPDH
85kDa
48kDa
63kDa
64kDa
198kDa
36kDa
C
IgG
ECM1-Ab
rECM1
rTSP-1
D
rADAMTS1
E
rMMP-2
F
rMMP-9
93kDa
G
20μM KRFK:
H
20μM KTFR:
I
TSP1
ADAMTS1
MMP2
MMP9
T1 A1 M2 M9 T1 A1 M2 M9
20μM KTFR
J
ECM1
ACTA2
COL1A1
COL3A1
TIMP1
Relative mRNA level
siECM1:
K
Con
KTFR
siECM1
COL3
TIMP-1
α-Tubulin
138 kDa
28 kDa
55 kDa
L
TGF-β1 LAP-D (R58)
DRAQ5
Merged
siCon
siECM1
siCon+KTFR
siECM1+KTFR
M
MMP activity
Fluor. intensity
20ng rECM1:
10ng MMP-2:
10ng MMP-9:

695 **Figure 4. ECM1 blocks TSP-1- and ADAMTS1-mediated LTGF-β1 activation via an**
696 **interaction with their respective KRFK/KTFR amino acid motifs and inhibits the**
697 **proteolytic activity of MMP-2 and MMP-9.**
698 **(A)** The concentration of active TGF-β (ng/ml) measured by SEAP activity assay from
699 conditioned MFB-F11 SN incubated with/without rLTGF-β1, rECM1 and/or LTGF-β1
700 activators. **(B)** Immunoprecipitation studies of ECM1 with MMP-2, MMP-9, ADAMTS1,
701 or TSP-1 in LX-2 HSCs cultured for 72h. An anti-human ECM1 antibody was used for
702 immunoprecipitation. MMP-2, MMP-9, ADAMTS1, and TSP-1 antibodies were used for
703 Western blotting. **(C-F)** *In vitro* pull-down assays of ECM1 and TSP-1, ADAMTS1,
704 MMP-2, or MMP-9. Recombinant proteins of ECM1, TSP-1, ADAMTS1, MMP-2, or
705 MMP-9 were incubated with protein A/G agarose. IgG or anti-human ECM1 antibody was
706 used for immunoprecipitation. ECM1, MMP-2, MMP-9, ADAMTS1, and TSP-1
707 antibodies were used for Western blotting. **(G)** The concentration of active TGF-β (ng/ml)
708 measured by SEAP activity assay from conditioned MFB-F11 SN incubated with/without
709 rLTGF-β1, rECM1 and/or KRFK peptide for 24h. **(H)** The concentration of active TGF-β
710 (ng/ml) measured by SEAP activity assay from conditioned MFB-F11 SN incubated
711 with/without rLTGF-β1 and/or KTFR peptide for 24h. **(I)** The concentration of active
712 TGF-β (ng/ml) measured by SEAP activity assay from conditioned MFB-F11 SN
713 incubated with rLTGF-β1 and the four mediators respectively combined the incubation
714 with/without KRFK peptide for 24h. **(J)** Relative mRNA levels of *ACTA2*, *COL1A1*,
715 *COL3A1*, and *TIMP1* in LX-2 HSCs transfected with siCon or si*ECM1*, incubated
716 with/without KTFR for 48h. **(K)** Protein expression of COL3 and TIMP1 in LX-2 HSCs
717 with the treatment as shown in the figure. **(L)** IF staining of TGF-β1 LAP-D (R58) in LX-
718 2 HSCs with the treatment as shown in the figure. Scale bar, 25 μm. **(M)** MMP activity
719 assay showing the enzymatic activity of MMP-2 and MMP-9 with/without rECM1
720 incubation. MMP Green Substrate was used as a control. For RT-qPCR, human PPIA was
721 used as an endogenous control. *P*-values were calculated by unpaired Student's t test. Bars
722 represent the mean ± SD. *, $P<0.05$; **, $P<0.01$.

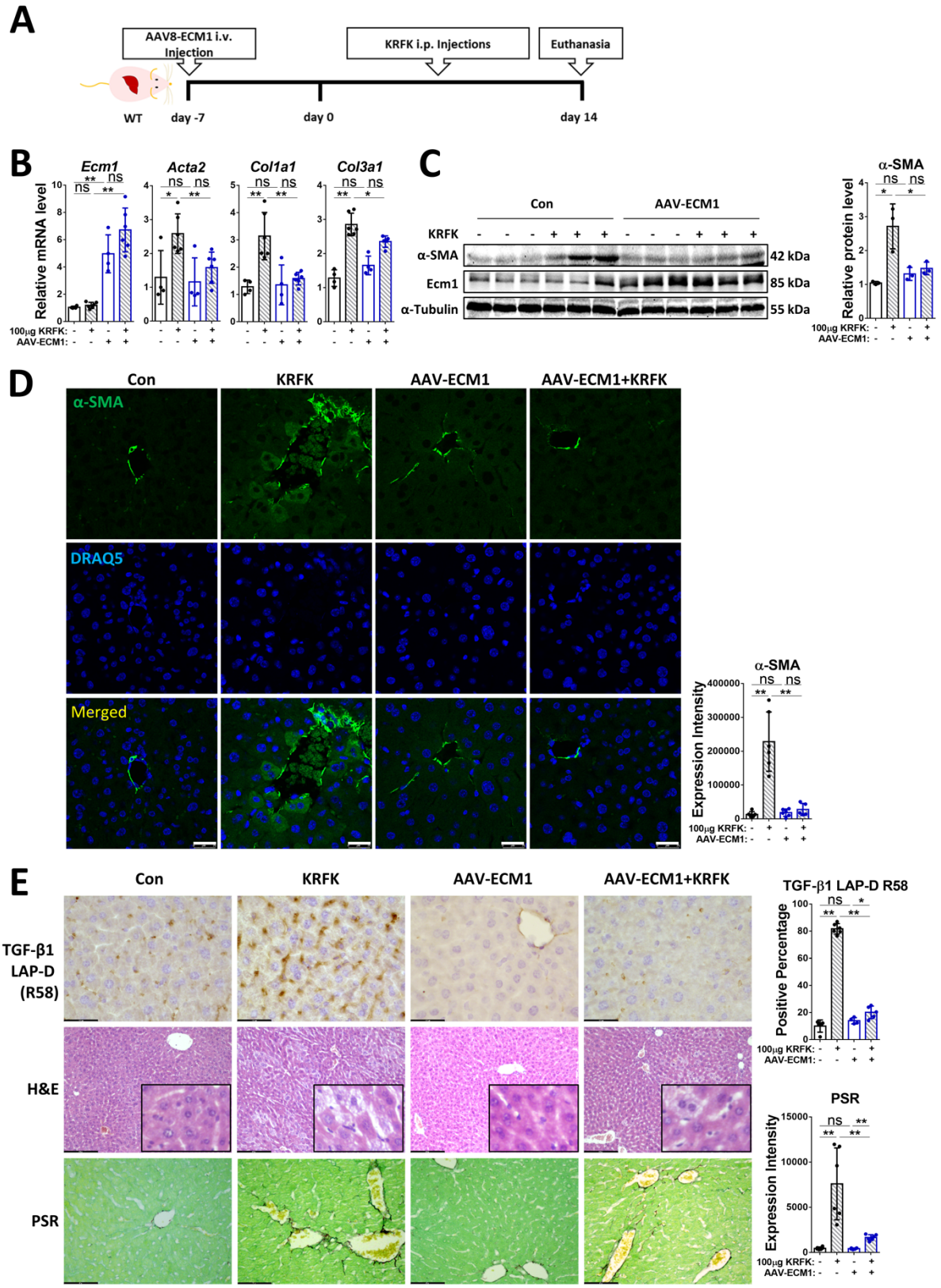
A
AAV8-ECM1 i.v. Injection
KRFK i.p. Injections
Euthanasia
WT
day -7
day 0
day 14
B
Ecm1
Acta2
Col1a1
Col3a1
Relative mRNA level
100μg KRFK:
AAV-ECM1:
C
Con
AAV-ECM1
KRFK
α-SMA
Ecm1
α-Tubulin
42 kDa
85 kDa
55 kDa
Relative protein level
D
Con
KRFK
AAV-ECM1
AAV-ECM1+KRFK
α-SMA
DRAQ5
Merged
Expression Intensity
E
TGF-β1 LAP-D (R58)
H&E
PSR
Positive Percentage
Expression Intensity

723 **Figure 5. ECM1 overexpression in the murine liver prevents KRFK peptide-induced**
724 **LTGF-β1 activation and subsequent hepatic fibrosis in WT mice.**
725 **(A)** Schematic illustration of *in vivo* experiment with AAV-ECM1 (i.v.) and KRFK
726 peptide (i.p.) injections of WT mice. **(B)** Relative RT-qPCR mRNA levels of *Ecm1*, *Acta2*,
727 *Col1a1*, and *Col3a1* in liver tissue from WT mice treated w/o AAV-ECM1, plus control or
728 KRFK peptide injection daily, for 14 consecutive days. **(C)** Protein levels of α-SMA in
729 liver tissue from WT mice treated with control or AAV-ECM1 followed by control or
730 KRFK peptide. **(D)** Representative images of IF stainings for α-SMA in liver tissue from
731 WT mice treated with control or AAV-ECM1 followed by control or KRFK peptide. Scale
732 bar, 25 μm. **(E)** Representative images of IHC stainings for TGF-β1 LAP-D R58, H&E,
733 and PSR staining in liver tissue from WT mice treated with control or AAV-ECM1
734 followed by control or KRFK peptide. Scale bar, 43.5, 174, 87 μm, respectively. For RT-
735 qPCR, mouse *Ppia* was used as an endogenous control. For Western blotting, α-Tubulin
736 was used as a loading control. P-values were calculated by unpaired Student's t test. Bars
737 represent the mean ± SD. *, $P<0.05$; **, $P<0.01$.

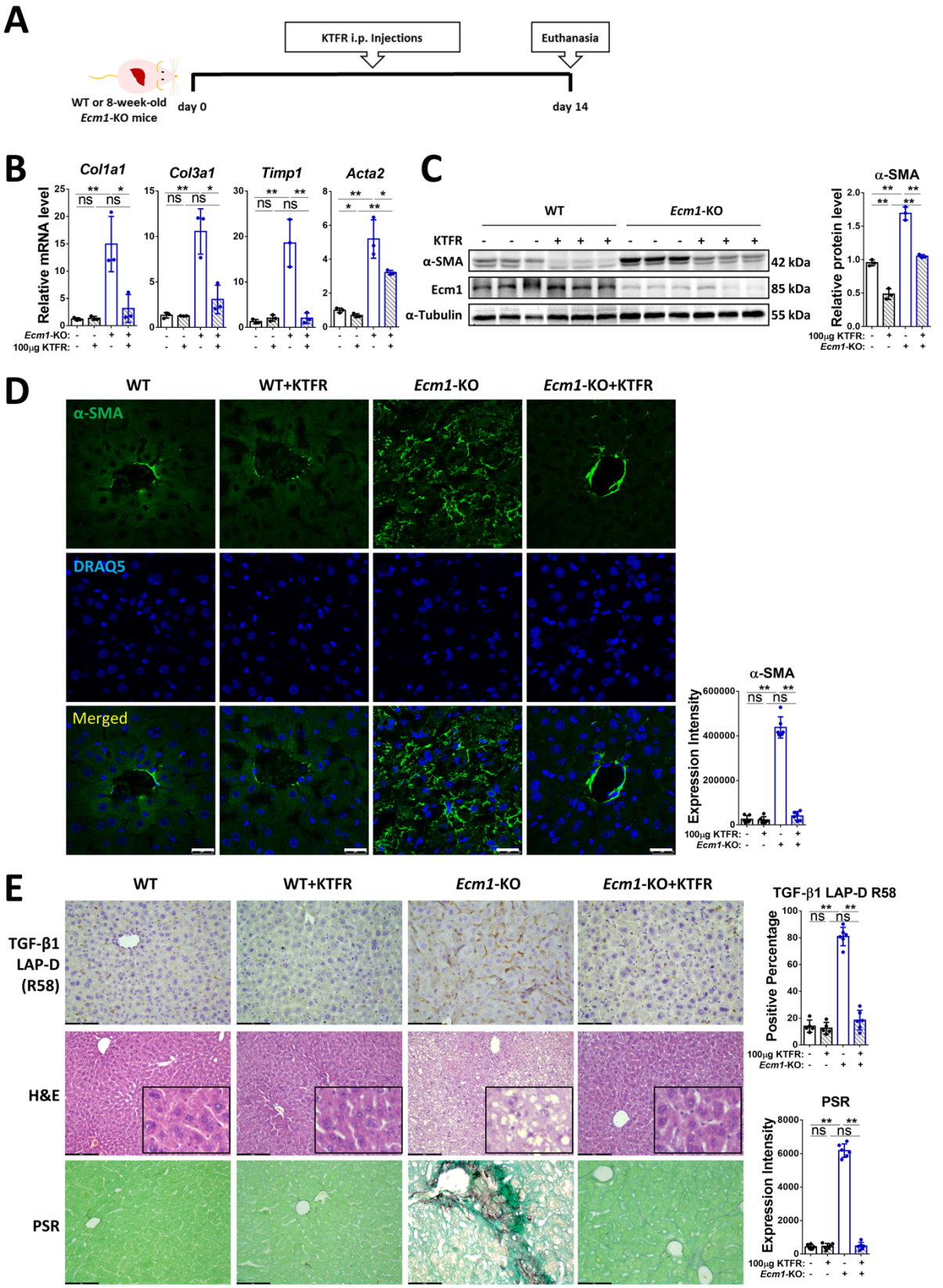
A
KTFR i.p. Injections
Euthanasia
WT or 8-week-old
Ecm1-KO mice
day 0
day 14
B
Col1a1
Col3a1
Timp1
Acta2
Relative mRNA level
ns
**
*
Ecm1-KO:
100μg KTFR:
C
WT
Ecm1-KO
KTFR
α-SMA
Ecm1
α-Tubulin
42 kDa
85 kDa
55 kDa
Relative protein level
100μg KTFR:
Ecm1-KO:
D
WT
WT+KTFR
Ecm1-KO
Ecm1-KO+KTFR
α-SMA
DRAQ5
Merged
Expression Intensity
100μg KTFR:
Ecm1-KO:
E
WT
WT+KTFR
Ecm1-KO
Ecm1-KO+KTFR
TGF-β1
LAP-D
(R58)
H&E
PSR
TGF-β1 LAP-D R58
Positive Percentage
PSR
Expression Intensity
100μg KTFR:
Ecm1-KO:

738 **Figure 6. KTFR peptide treatment rescues liver injury in *Ecm1*-KO mice.**
739 **(A)** Schematic illustration of *in vivo* experiments with KTFR peptide injections (i.p.) into
740 WT and *Ecm1*- KO mice. **(B)** Relative mRNA levels of *Col1a1*, *Col3a1*, *Timp1*, and
741 *Acta2* in liver tissue from WT and *Ecm1*-KO mice injected with control or KTFR peptide
742 daily, for 14 consecutive days. **(C)** Protein levels of α-SMA in liver tissue from WT and
743 *Ecm1*-KO mice injected with control or KTFR peptide. **(D)** Representative images of IF
744 stainings of α-SMA in liver tissue from WT and *Ecm1*-KO mice injected with control or
745 KTFR peptide. Scale bar, 25 μm. **(E)** Representative images of IHC stainings for TGF-β1
746 LAP-D R58, H&E, and PSR staining in liver tissue from WT and *Ecm1*-KO mice injected
747 with control or KTFR peptide. Scale bar, 43.5, 174, 87 μm, respectively. For RT-qPCR,
748 mouse *Ppia* was used as an endogenous control. For Western blotting, α-Tubulin was used as a
749 loading control. *P*-values were calculated by unpaired Student's t test. Bars represent the
750 mean ± SD. *, $P<0.05$; **, $P<0.01$.

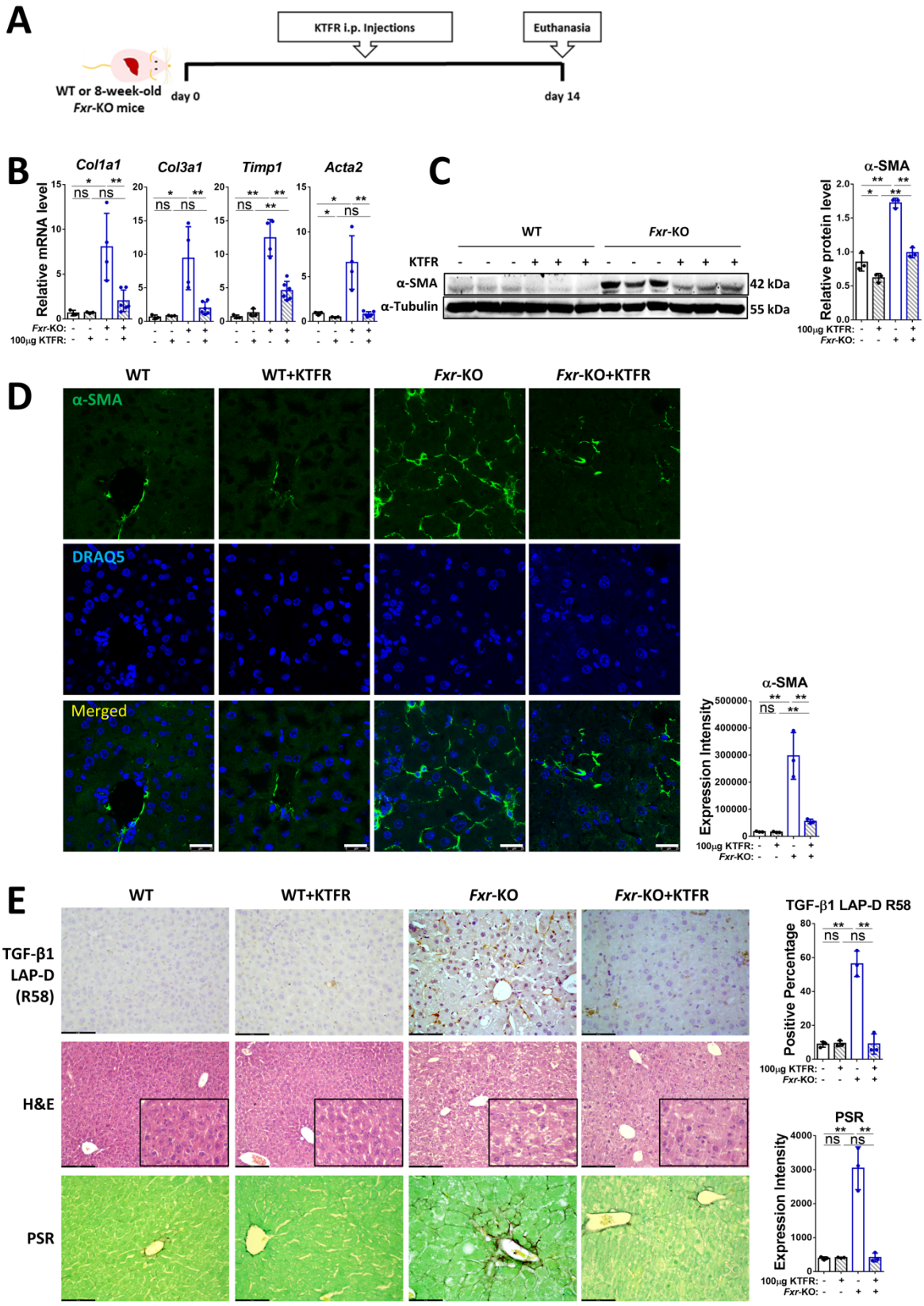
A
KTFR i.p. Injections
Euthanasia
WT or 8-week-old
Fxr-KO mice
day 0
day 14
B
Col1a1
Col3a1
Timp1
Acta2
Relative mRNA level
Fxr-KO:
100μg KTFR:
C
WT
Fxr-KO
KTFR
α-SMA
α-Tubulin
42 kDa
55 kDa
α-SMA
Relative protein level
D
WT
WT+KTFR
Fxr-KO
Fxr-KO+KTFR
α-SMA
DRAQ5
Merged
Expression Intensity
E
TGF-β1
LAP-D
(R58)
H&E
PSR
TGF-β1 LAP-D R58
Positive Percentage

751 **Figure 7. KTFR peptide treatment rescues liver injury in *Fxr*-KO mice.**
752 **(A)** Schematic illustration of *in vivo* experiments with KTFR peptide injections (i.p.) into
753 WT and *Fxr*- KO mice. **(B)** Relative mRNA levels of *Col1a1*, *Col3a1*, *Timp1*, and *Acta2*
754 in liver tissue from WT and *Fxr*-KO mice injected with control or KTFR peptide for 14
755 consecutive days. **(C)** Protein levels of α-SMA in liver tissue from WT and *Fxr*-KO mice
756 injected with control or KTFR peptide. **(D)** Representative images of IF stainings of α-
757 SMA in liver tissue from WT and *Fxr*-KO mice injected with control or KTFR peptide.
758 Scale bar, 25 μm. **(E)** Representative images of IHC stainings for TGF-β1 LAP-D R58,
759 H&E, and PSR staining in liver tissue from WT and *Fxr*-KO mice injected with control or
760 KTFR peptide. Scale bar, 43.5, 174, 87 μm, respectively. For RT-qPCR, mouse *Ppia* was
761 used as an endogenous control. For Western blotting, α-Tubulin was used as a loading control.
762 *P*-values were calculated by unpaired Student's t test. Bars represent the mean ± SD. *,
763 $P<0.05$; **, $P<0.01$.

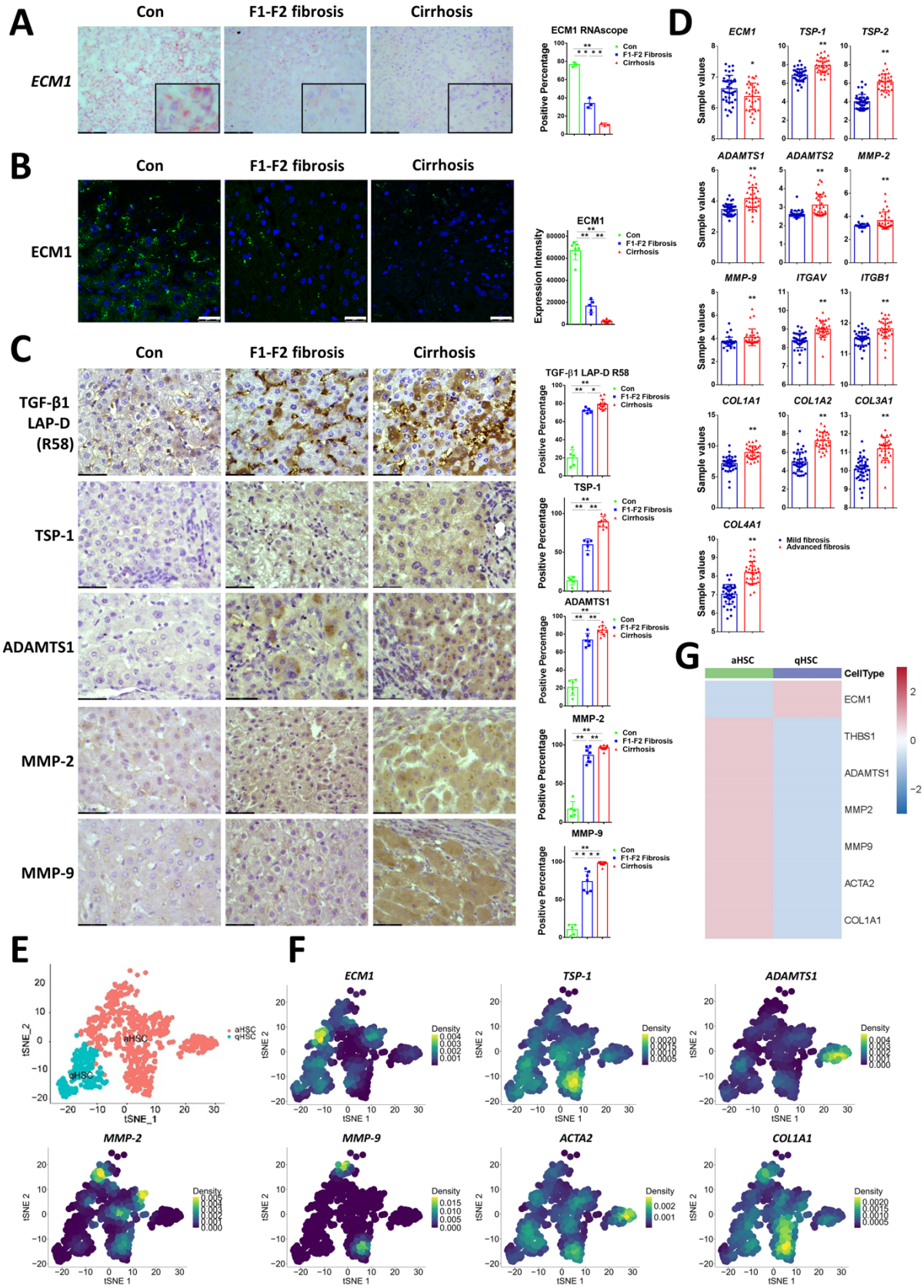
A
Con
F1-F2 fibrosis
Cirrhosis
ECM1
ECM1 RNAscope
Positive Percentage
Con
F1-F2 Fibrosis
Cirrhosis
B
ECM1
Expression Intensity
C
TGF-β1 LAP-D (R58)
TSP-1
ADAMTS1
MMP-2
MMP-9
TGF-β1 LAP-D R58
D
ECM1
TSP-1
TSP-2
ADAMTS1
ADAMTS2
MMP-2
MMP-9
ITGAV
ITGB1
COL1A1
COL1A2
COL3A1
COL4A1
Sample values
Mild fibrosis
Advanced fibrosis
G
aHSC
qHSC
CellType
ECM1
THBS1
ADAMTS1
MMP2
MMP9
ACTA2
COL1A1
E
tSNE_1
tSNE_2
aHSC
qHSC
F
ECM1
TSP-1
ADAMTS1
MMP-2
MMP-9
ACTA2
COL1A1
tSNE 1
tSNE 2
Density

764 **Figure 8. Decreased ECM1 and increased mediators of L-TGF-β1 activation are**
765 **associated with progressing fibrosis in CLD patients.**
766 **(A)** Representative *ECM1* RNAscope data in liver tissue from control, F1-F2 fibrosis, and
767 cirrhosis liver tissue. Scale bar, 87 μm. **(B)** Representative images of IF stainings for
768 ECM1 in control, F1-F2 fibrosis, and cirrhosis liver tissue. DRAQ5 was used for nuclear
769 staining. Scale bar, 25 μm. **(C)** Representative images of IHC staining for TGF-β1 LAP-D
770 R58, TSP-1, ADAMTS1, MMP-2, and MMP-9 in control, F1-F2 fibrosis, and cirrhosis
771 liver tissue. Scale bar, 43.5 μm. **(D)** mRNA expression of *ECM1*, LTGF-β1 activators, and
772 fibrotic collagens in liver tissue from patients with F1-2 fibrosis or cirrhosis, extracted
773 from GEO DataSets GSE49541. **(E)** UMAP visualization of isolated hepatic stellate cells
774 from GSE174748. **(F, G)** Density plots and heatmaps show the relative expression of
775 target genes in scRNAseq of HSC subsets from GSE174748. Quantification of stainings
776 was performed using Image J (National Institute of Health, Bethesda, MD). *P*-values were
777 calculated by unpaired Student's t test. Bars represent the mean ± SD. *, $P<0.05$; **,
778 $P<0.01$.

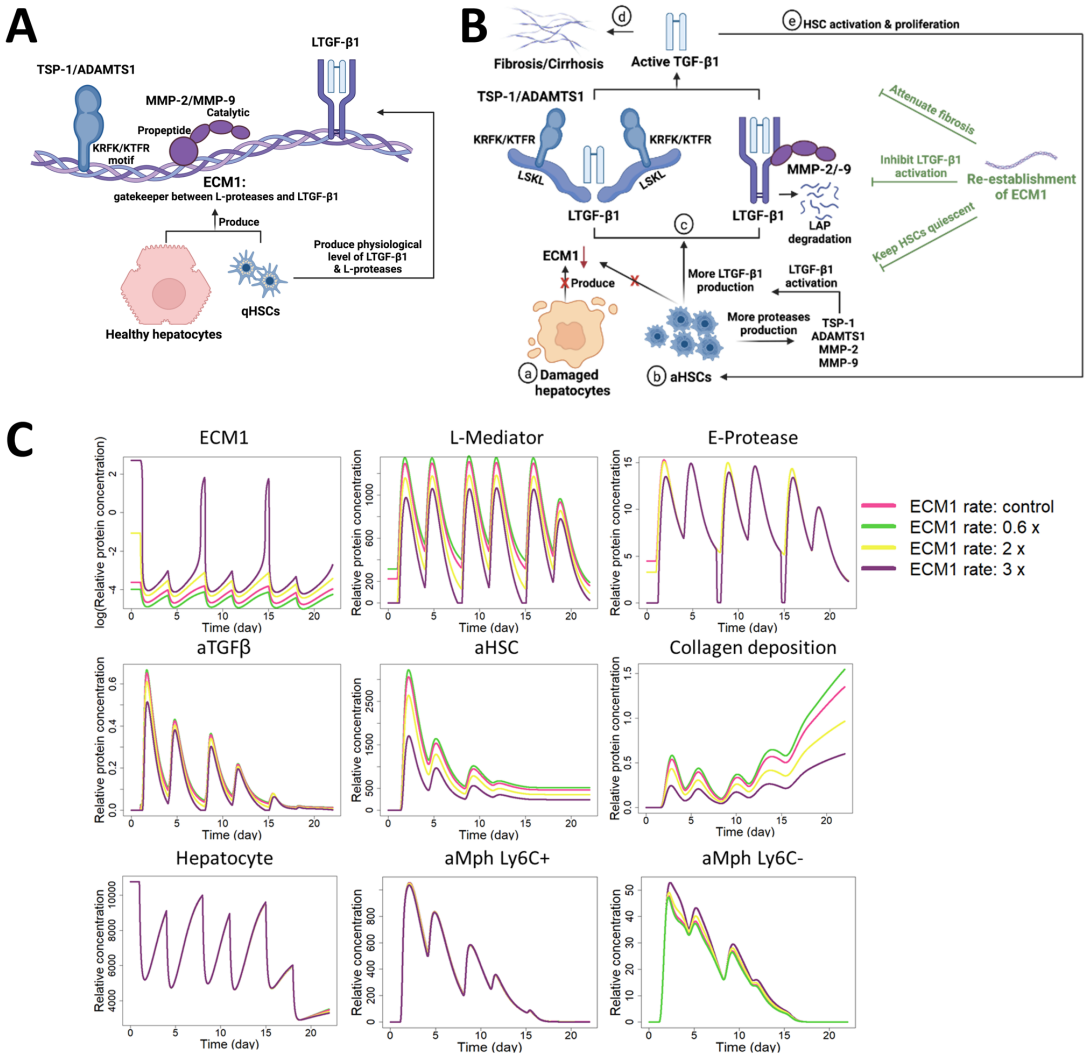
A
TSP-1/ADAMTS1
LTGF-β1
MMP-2/MMP-9
Catalytic
Propeptide
KRFK/KTFR motif
ECM1:
gatekeeper between L-proteases and LTGF-β1
Produce
Produce physiological level of LTGF-β1 & L-proteases
qHSCs
Healthy hepatocytes
B
Fibrosis/Cirrhosis
Active TGF-β1
HSC activation & proliferation
TSP-1/ADAMTS1
KRFK/KTFR
LSKL
LTGF-β1
MMP-2/-9
LAP degradation
Attenuate fibrosis
Inhibit LTGF-β1 activation
Re-establishment of ECM1
Keep HSCs quiescent
ECM1
Produce
More LTGF-β1 production
LTGF-β1 activation
More proteases production
TSP-1
ADAMTS1
MMP-2
MMP-9
Damaged hepatocytes
aHSCs
C
ECM1
L-Mediator
E-Protease
aTGFβ
aHSC
Collagen deposition
Hepatocyte
aMph Ly6C+
aMph Ly6C-
log(Relative protein concentration)
Relative protein concentration
Relative concentration
Time (day)
ECM1 rate: control
ECM1 rate: 0.6 x
ECM1 rate: 2 x
ECM1 rate: 3 x

Figure 9. ECM1's role in maintaining liver tissue homeostasis in healthy livers and its dysregulation during chronic liver disease.

(A) In healthy livers, ECM1 from healthy hepatocytes and quiescent HSCs prevents excessive LTGF-β1 activation by TSP-1 and ADAMTS1 through interacting with their respective KRFK and KTFR motifs and binding to MMP-2 an MMP-9, limiting their enzymatic activity thus keeping the TGF-β1 inactive within its ECM-deposited latent complex (LTGF-β1). **(B)** During CLD, (a) damaged hepatocytes fail to maintain ECM1 expression and production which results in (b) increased and detrimental LTGF-β1 activation via (c) conformational changes in the LAP molecule caused by TSP-1 and ADAMTS1 or via direct proteolysis of the LAP molecule as caused by MMP-2 and MMP-9. Increased levels of active TGF-β1 promote (d) the accumulation of excessive extracellular matrix and cause (e) HSC activation, thus resulting in (progressive) hepatic fibrosis. Intriguingly, ectopic ECM1 expression (rECM1/v-ECM1) inhibits TSP-1, ADAMTS1, MMP-2 and MMP-9-mediated LTGF-β1 activation and attenuates subsequent hepatic fibrosis (Right in green). **(C)** Simulation of chronic liver injury. Simulation of 4 doses of CCl_4 (at day 1, 4, 8, 11) for 15 days under four different ECM1 production rates: the control k_1^{HC}, k_1^{HH}, 0.6-fold of the control $0.6 \times k_1^{HC}, 0.6 \times k_1^{HH}$, 2-fold of the control $2 \times k_1^{HC}, 2 \times k_1^{HH}$, and 3-fold of the control $3 \times k_1^{HC}, 3 \times k_1^{HH}$. The first dose of CCl_4 is injected at day 1 when the system is in a healthy steady state. Shown are the relative concentrations of ECM1, L-Mediator and E-Protease (first row), active TGF-β1 (aTGF-β1), activated HSC (aHSC), collagen deposition (second row), hepatocytes, Ly6C+ and Ly6C- macrophages (aMph) (third row) as a function of time for four different ECM1 production rates.